Norwegian Meteorological Institute

MET report

no. 19/2013
Numerical Weather Prediction

The IASI moisture channel impact study in HARMONIE for August-September 2011

Trygve Aspelien, Roger Randriamampianina, Harald Schyberg, Frank Thomas Tveter and Ole Vignes

Norwegian Meteorological Institute

MET report

Title The IASI moisture channel impact study in HARMONIE for August-September 2011	**Date** 1 November 2013
Section Numerical Weather Prediction	**Report no.** 19
Author(s) Trygve Aspelien, Roger Randriamampianina, Harald Schyberg, Frank Thomas Tveter and Ole Vignes	**Classification** Free
	ISSN 1503-8025
	e-ISSN 1503-8025
Client(s) Norwegian Space Centre/MET	**Client's reference** JOP 07.12.3

Abstract

The present report describes an experiment with the HARMONIE NWP system to test the impact of IASI moisture channels at MET Norway. The model setup for assimilation of these data was developed at MET in 2012. The model setup and channel usage is described, along with impact experiments. A slight net positive impact from IASI moisture channels is seen in the precipitation verification, but the impact is highly variable and situation dependent. The moisture increments from IASI seem not to affect the average precipitation or the large-scale precipitation structures significantly, but it affects the positioning of precipitation cells.

Keywords

IASI, Data assimilation, Numerical Weather Prediction

Disiplinary signature	Responsible signature

Postal address P.O.Box 43, Blindern NO-0313 OSLO Norway
Office Niels Henrik Abelsvei 40
Telephone +47 22 96 30 00
Telefax +47 22 96 30 50
e-mail: met@met.no **Internet:** met.no
Bank account 7694 05 00628
Swift code DNBANOKK

Contents

1 Introduction

IASI is the present satellite sounding sensor which seems to have the largest potential per sensor in bringing benefit to numerical weather prediction (NWP). The Norwegian Meteorological Institute (MET Norway) runs regional NWP models, which play an important role in the forecasting services. The HARMONIE (HIRLAM Aladin Regional/Meso-scale Operational NWP In Europe) model system will be the main future regional NWP system of MET Norway, and this includes a three-dimensional variational (3D-Var) data assimilation system. A first implementation of IASI temperature assimilation in HARMONIE 3D-Var has already been done and has proven to give positive impact in a limited number of Polar Low situations (see Randriamampianina et al, 2011). An ongoing project co-funded by the Norwegian Space Centre focuses on further optimization of the data usage and impact, with special focus on including moisture channels for assimilation.

This report first presents monitoring results of the observations versus simulated observations using data from the HARMONIE forecasting system. The radiances were simulated with RTTOV (Radiative Transfer for TOVS) radiative transfer model (Matricardi et al., 2004), which also was used as observation operator in the assimilation trials described later here. In general different NWP models have different resolution, area coverage and error characteristics, which leads to different statistics datasets for the comparison of model-simulated radiances and real IASI data.

The statistics from this dataset has served as an aid in choosing which moisture channels to assimilate in the assimilation trial, which is also described in this report.

2 IASI data stream

IASI data used here come from an operational input data flow from EUMETSAT's real time dissemination service. IASI has 8461 channels, of which we extract 366 for potential use in HARMONIE 3D-Var. In the selection of the 366 channels for monitoring, we followed the choice for channels done by Collard and McNally (2009).

The processing takes place in cooperation with the MET operational department, who stores the data. The data volumes are large, 3 minutes of a passage is around 30 Mb of data (all 8461 channels are present). A program was written to extract the subset of channels (currently 366), and to pick data only for the geographical area of interest (the model domain is shown on Fig. 1). This reduced volumes to be around 60-70 Mb/day. Data have been stored on disk since May 22, 2011.

For pre-processing and assimilation, code modules from ECMWF, Meteo-France and EUMETSATs NWP-SAF (Satellite Application Facility) were available which were adopted to the HARMONIE system. Part of this work was done during the implementation of the IASI temperature sensitive channels assimilation performed at MET Norway in the frame of the IPY-THORPEX project (Randriamampianina et al, 2011).

3 Channel monitoring statistics and channel selection

HARMONIE was first set up to do monitoring of IASI in passive mode. Observation data for a period of about one month (May 22 – June 25 2011, 4 assimilation cycles/day) was transferred to the supercomputer, which allowed us to assimilate the IASI data in a passive way (this means that the data are entering the assimilation procedure, but they do not influence the final analysis) in the Harmonie 3D-Var system (pre-processing, screening, minimization).and IASI data was fed to the Harmonie 3D-Var system (preprocessing, screening, minimization).

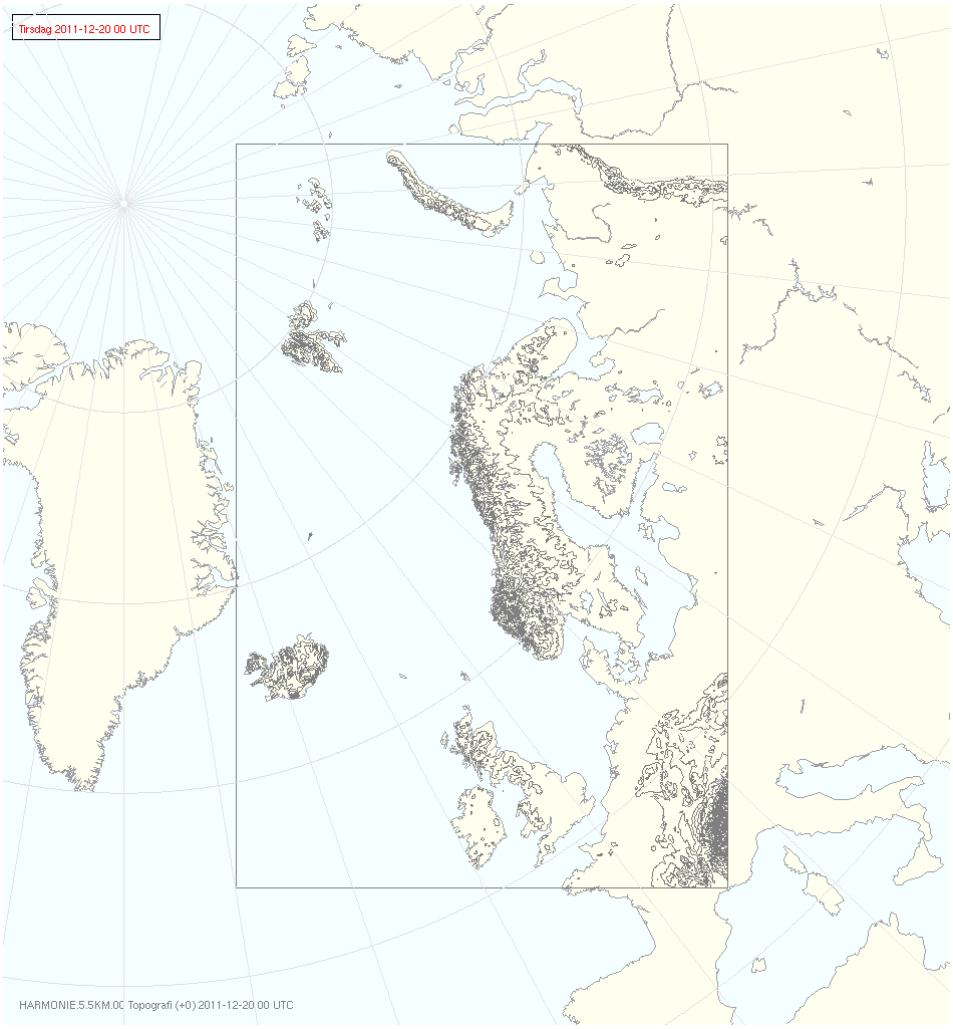

Figure 1: The domain of the HARMONIE model used in this study. Contours show the coastlines and the model topography.

All the monitored channels were analyzed in terms of deviation between the simulated value (using HARMONIE profiles as input to RTTOV) and the actual observed radiances. For the statistics a check for cloud contamination was done, and only observations passing as non-cloudy from this screening are shown. In Figures 2-4 we present examples of timeseries plots for such statistics for a few selected channels.

Temperature channels

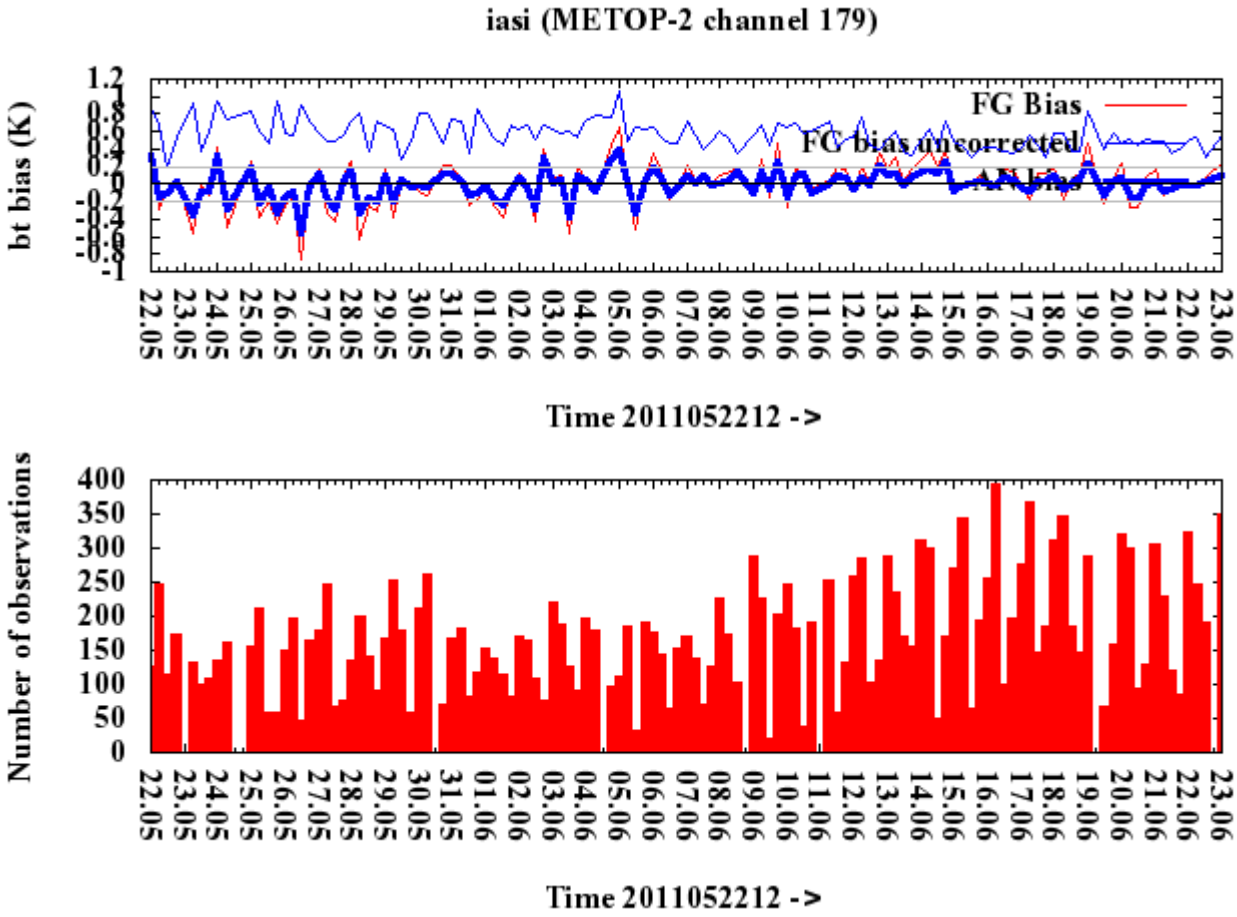

Figure 2: Monitoring statistics for channel 179 (temperature upper troposphere)

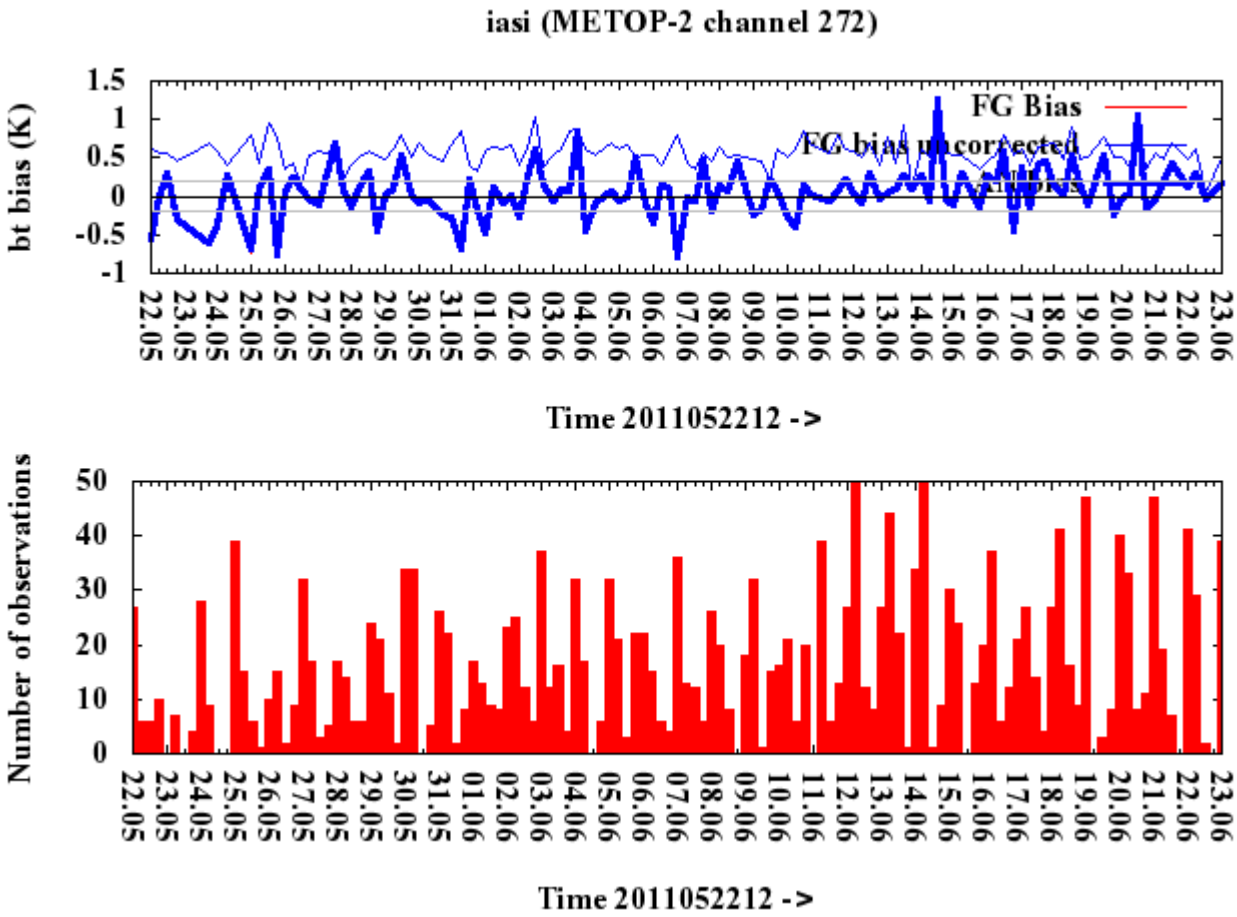

Figure 3: Monitoring statistics for Channel 272 (temperature lower troposphere).

Moisture channels

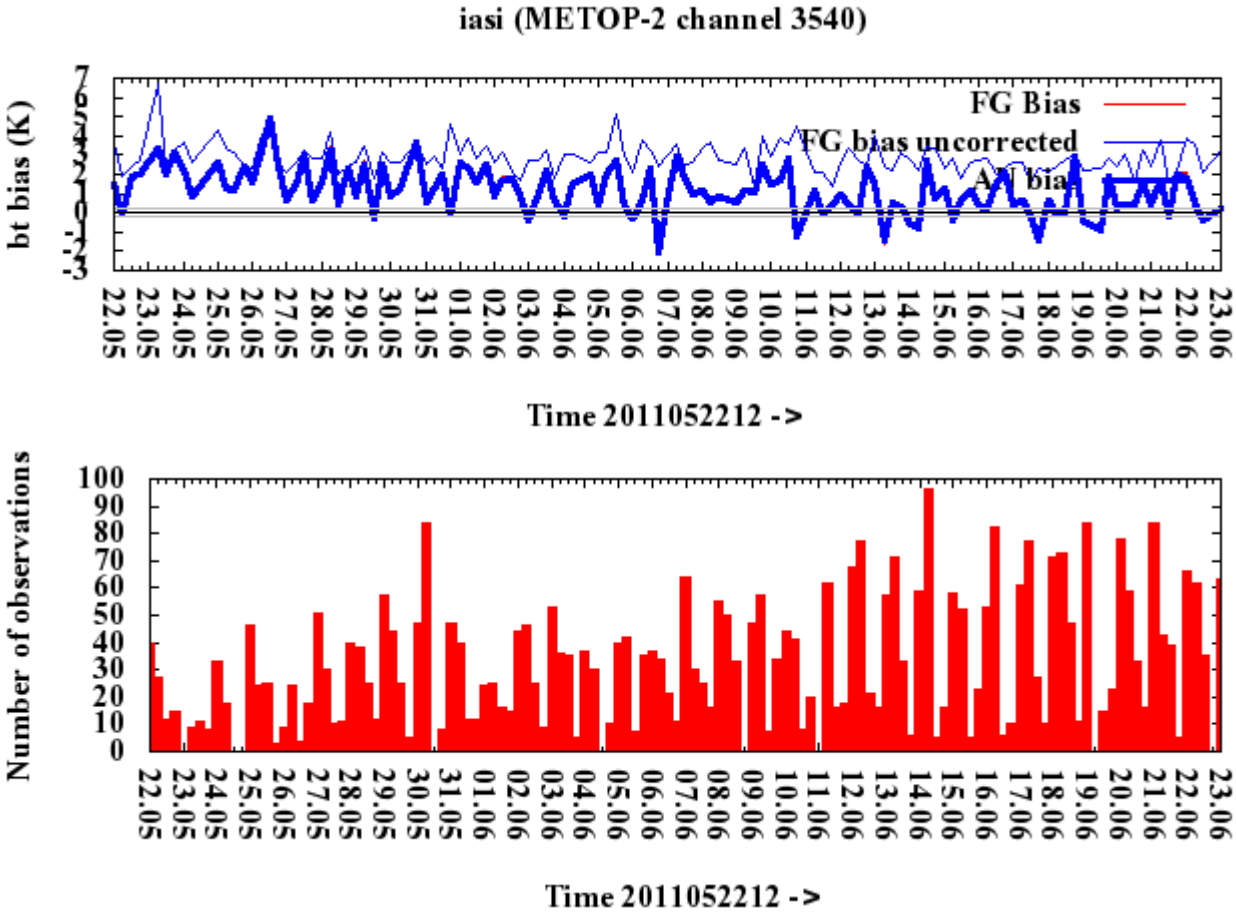

Figure 4: Monitoring statistics for channel 3540 (moisture mid troposphere)

The sensitivity of of all the 366 pre-selected channels in term of increment statistics (observed – modeled radiances) has been studied, and this has resulted in a further reduction of the number of usable/active channels. The channels selected for assimilation were considered separately for land and sea and also for the four assimilation times (0, 6, 12 and 18 UTC)..

The temperature channels selected for assimilation are given in Table 1, and the moisture channel usage is presented in Table 2.

The active moisture sensitive channels for assimilation were also selected from the 366 pre-selected channels with the same technique described above. The selected channels are mainly sensitive to upper tropospheric atmospheric thicknesses, see Table 2. Such a choice is "conservative" in the sense that potential cloud detection problems are smaller, but also in that the water vapor content of the atmosphere at these upper-tropospheric levels are quite small, since vapour content typically decreases approximately exponentially with height, and the bulk of water vapor is in the lower troposphere. Channels further down which were not used here could have provided much more information content on the bulk of the atmospheric vapour, but it would come at a risk of larger quality or interpretation problems coming from cloud and surface contributions to the signal which could not be accounted for by the use of the radiative transfer scheme with the model background.

In total 15 moisture channels were selected for assimilation. The number of selected channels over land and sea is slightly different for the 4 cycles (00, 06, 12, 18 UTC).

Channel no	Approx Peak Level (hPa)	Land 00	Land 06	Land 12	Land 18	Sea 00	Sea 06	Sea 12	Sea 18
Tot used		10	42	45	50	63	60	62	59
49	50		X	X	X	X	X	X	X
51	80					X	X	X	X
55	60		X	X	X	X	X	X	X
59	30					X	X	X	X
61	50		X	X	X	X	X	X	X
63	90	X	X	X	X	X	X	X	X
66	40	X	X	X	X	X	X	X	X
74	40		X	X	X	X	X	X	X
79	40		X		X	X	X	X	X
81	40		X	X	X	X	X	X	X
83	60		X	X	X	X	X	X	X
85	60		X	X	X	X		X	X
87	60					X	X	X	X
89	30		X	X	X	X	X	X	X
101	30					X	X	X	X
104	50		X	X	X	X	X	X	X
106	30		X	X	X	X	X	X	X
109	90		X	X	X	X	X	X	X
111	50			X	X	X	X	X	X
116	90		X	X					
119	30		X	X	X	X	X	X	X
122	80			X		X	X	X	X
125	30		X		X	X	X	X	X
128	80			X	X	X	X	X	X
131	20		X			X			
133	50	X	X	X	X	X	X	X	X
135	80			X		X	X	X	X
138	30	X	X	X	X	X	X	X	X
141	80			X	X	X	X	X	X
144	30			X	X				
146	50		X	X	X	X	X	X	X
148	80			X	X	X	X	X	X
154	100		X	X	X	X	X	X	X
159	80		X	X	X	X	X	X	X
161	100				X	X	X	X	X
163	40		X		X				
165	60		X	X	X	X	X	X	X
167	100		X			X	X	X	X
170	40		X	X					
173	120			X	X	X	X	X	X
178	100			X	X	X	X	X	X
179	150			X	X	X	X	X	X
180	150				X	X	X	X	X
183	50		X		X	X	X	X	X
185	150		X	X	X	X	X	X	X
187	150			X	X	X	X	X	X

189	40		X	X	X	X	X	X	X
191	150		X			X	X	X	X
193	180		X		X	X	X	X	X
195	50		X	X	X	X	X	X	X
197	150		X		X	X	X	X	X
199	200		X		X	X	X	X	X
201	100		X	X	X	X	X	X	X
203	100		X	X	X	X	X	X	X
205	230		X	X	X	X	X	X	X
207	180		X	X	X	X	X	X	X
210	180			X	X	X	X	X	X
214	160		X	X	X	X	X	X	X
217	250	X							
219	270	X			X	X	X	X	X
222	210			X	X	X	X	X	X
224	250	X							
228	250				X	X	X	X	X
232	320		X						
299	250					X	X	X	X
301	50					X	X	X	X
303	30					X	X	X	X
347	500		X						
3378	300	X							
3555	250	X				X	X	X	
3599	300	X					X		
3661	250			X		X		X	
4032	250			X		X		X	

Table 1: Overview of temperature channel usage

Channel number	**Typical approximate peak level (hPa)**
3448	250
3450	250
3452	300
3491	300
3506	300
3555	300
3575	300
3577	250
3580	250
3582	300
3589	300
3653	250
3658	300
3661	300
4032	250

Table 2: Moisture channels used along with typical peak pressure level in the atmosphere

4 Model and experiment setup

IASI temperature channel assimilation is well developed, and has also been demonstrated to give a positive impact on the HARMONIE model used at MET Norway (see Randriamampianina et al, 2011). Presently several NWP centres has focussed more attention on the assimilation of moisture sensitive channels. In the following we describe an initial experiment with the HARMONIE system study the impact of IASI moisture channels on a limited area model (LAM) in use at met.no. The model setup for assimilation of these data was developed at MET Norway in 2012.

4.1 The HARMONIE model implementation

The NWP model applied in this study (see the domain on Fig. 1) is a 5.5 km horizontal resolution version of the HARMONIE hydrostatic model with the so called ALARO physics package running in experimental mode in 2012. It is similar to a pre-operational version of the model which is now run routinely and was available to forecasters. HARMONIE is now becoming the operational model at MET Norway (in a version with even higher resolution and a different physics package, AROME). The HARMONIE system shows encouraging verifications results compared to the earlier regional operational models applied in the forecasting service.

4.2 Experiment setup

In this experiment a parallel impact trial with moisture channels was set up for a late summer experimental period covering 15 Aug – 15 Sep 2011. A reference run assimilated conventional observations and satellite data including IASI temperature channels, while the experiment run assimilated the same data, and in addition the selected moisture channels.

A late summer period was chosen because a main goal is to study the potential impact of IASI radiances on our predicting capabilities of clouds and precipitation, and during late summer typically we typically observe high amounts of water vapour content in the atmosphere with both significant convective shower activity and frontal passages.

4.3 Bias monitoring

A bias correction procedure has proven necessary to correct for systematic errors in the model, observations, in the observation operator and effects not described by the observation operator.

The bias between the IASI channel observations and the first guess model equivalent is modelled as a sum of predictors multiplied by a set if coefficients. The following predictor definitions are available:

p0 : 1 (constant)
p1 : 1000-300hPa thickness
p2 : 200-50hPa thickness
p3 : T_skin
p4 : total column water
p5 : 10-2hPa thickness
p6 : 50-5hPa thickness
p7 : surface wind speed
p8 : nadir viewing angle

p9 : nadir view angle **2
p10: nadir view angle **3
p11: nadir view angle **4
p12: cos solar zen angle
p13: solar elevation
p14: TMI diurnal bias
p15: land or sea ice mask
p16: view angle (land)
p17: view angle **2 (land)
p18: view angle **3 (land)

The following predictors from the list are used for the IASI WV channels: p0,p1,p2,p5, p6, p8, p9, p10.

Variational bias correction is applied to the Metop-2 IASI water vapour channels. In this approach the coefficients are put into the control vector and adjusted during the minimisation. The new estimated coefficients are used as first estimate for the next day assimilation. Here we update and cycle the coefficients for the radiance bias correction suggested in Randriamampianina et al. (2011), which means that the coefficients are updated daily for each assimilation cycle (00, 06, 12, and 18 UTC).

The following image plot (Figure 5) shows the bias in channel 4032 during the experiment period, before and after Variational bias-correction. Appendix A gives a more complete overview of the bias in the different IASI WV channels used in the experiment.

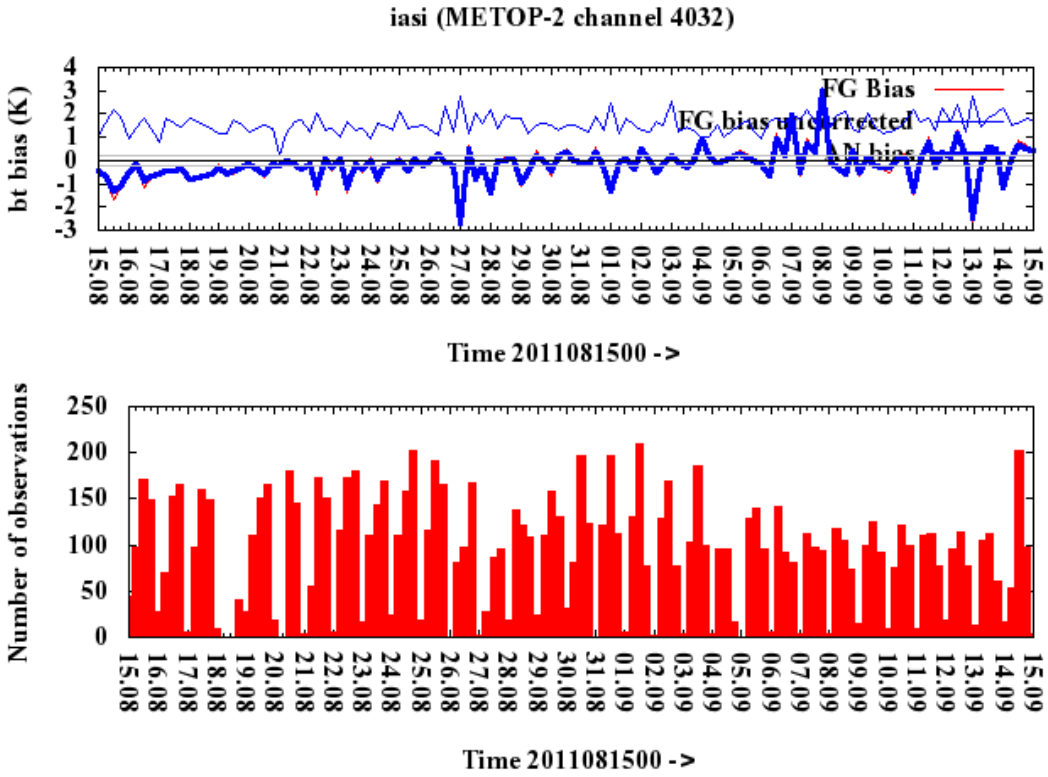

Figure 5: Example showing a bias plot for a particular channel (channel 4032) throughout the experiment period along with number of active observations available within the model domain for each assimilation time

4.4 Typical geographical coverage and example of usage in assimilation

Throughout the experiment period the observations which were rejected due to thinning or quality control and those available to the assimilation were monitored with a software package. Some typical results from this monitoring are presented in this section.

Figure 6 shows as an example the use of IASI channel 4032 at a certain time in the experiment period.

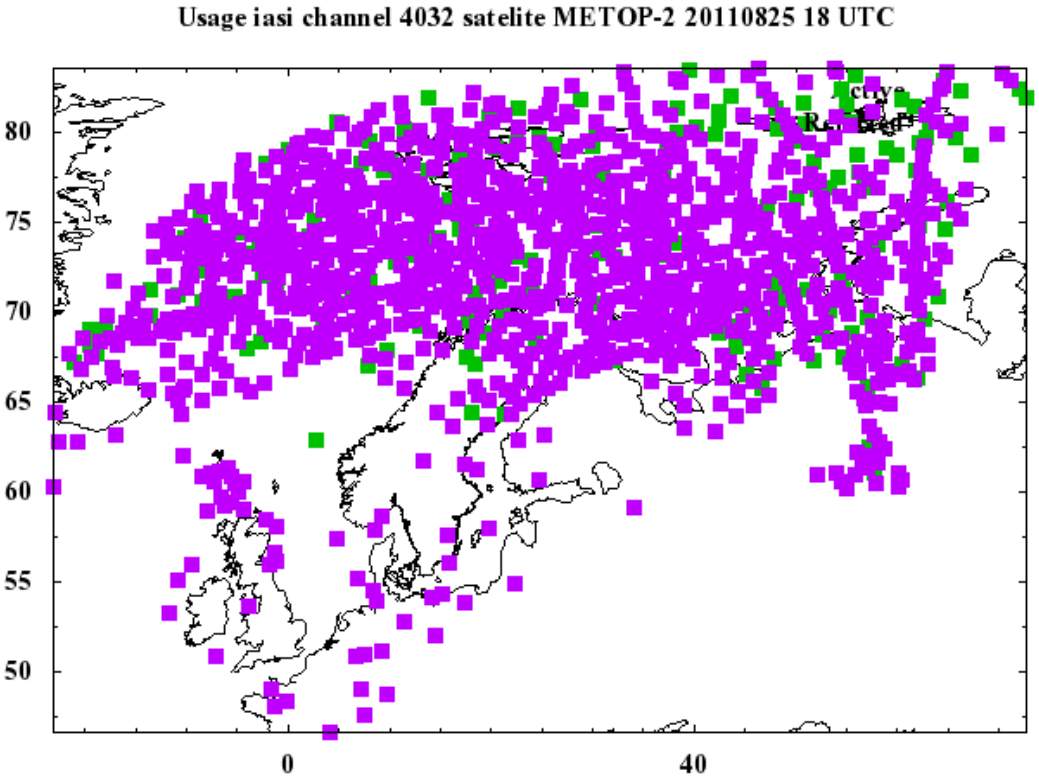

Figure 6: IASI ch 4032 observations available at 2011/08/25 18UTC. The green dots represent observations that are accepted (active) radiances for assimilation.

Figure 7 shows the active observations considered for assimilation at the same time.

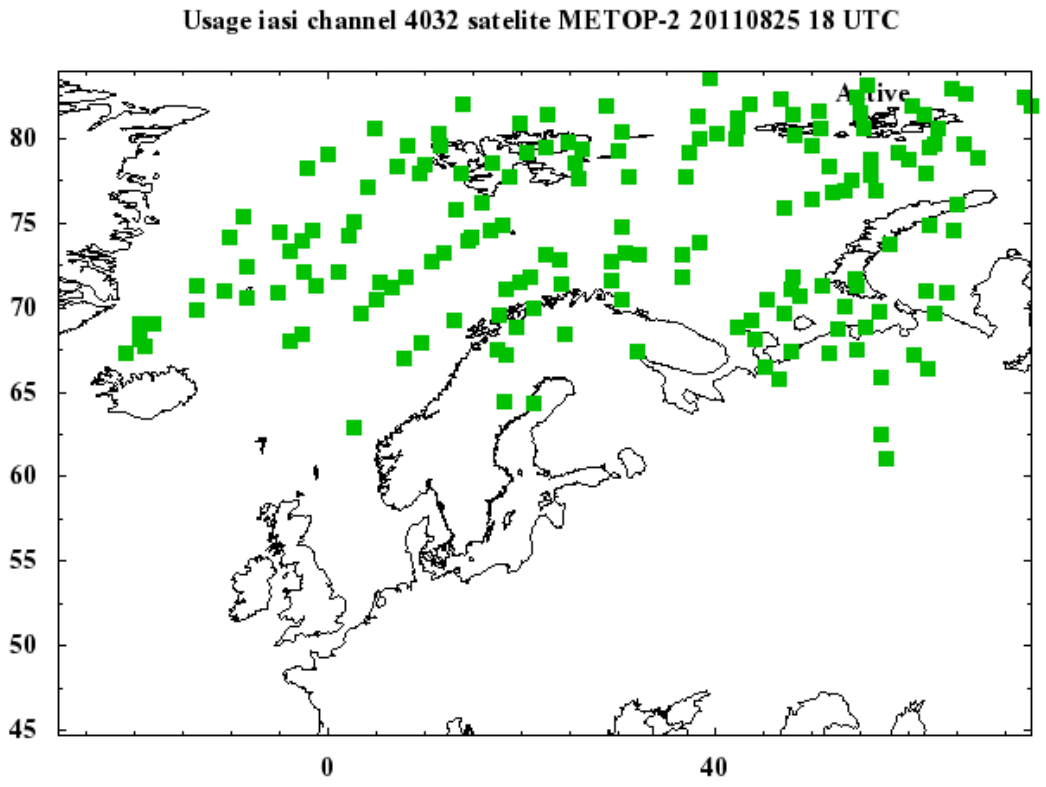

Figure 7: IASI ch 4032 observations input to the assimilation at 2011/08/25 18UTC

Figure 8 shows the bias correction applied to the active data.

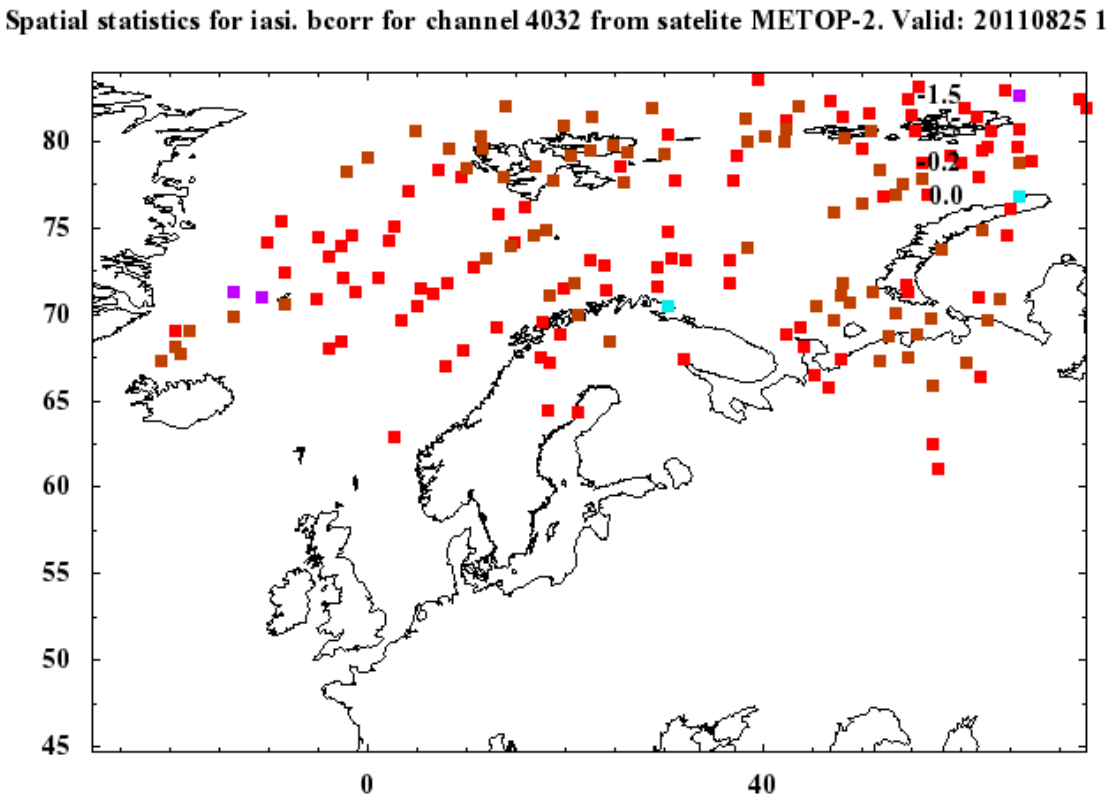

Figure 8: IASI ch 4032 magnitude of bias correction at 2011/08/25 18 UTC

Figure 9 shows the geographical distribution of the departure (increment) between the IASI channel 4032 observations and the first guess equivalent using the initial bias correction coefficients.

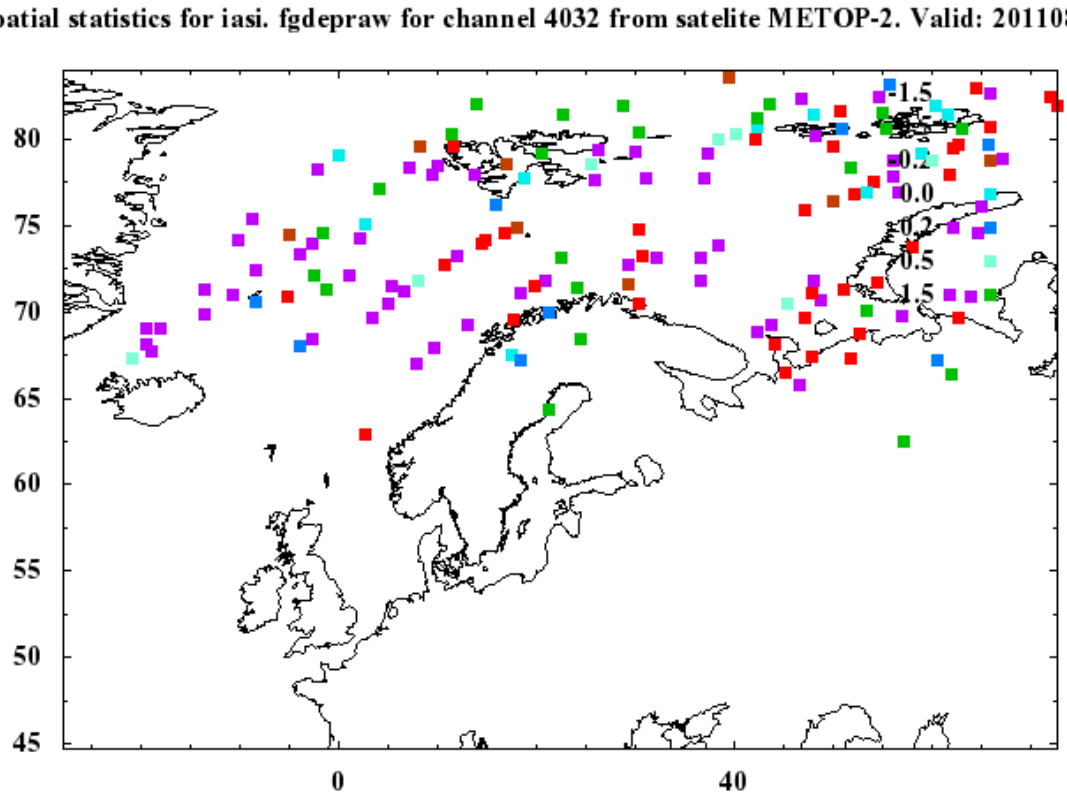

Figure 9: Departures from first guess field (a 6 hours forecast) before the bias correction for ch 4032 at same time as previous figures.

Figure 10 shows the geographical distribution of the departure between the IASI channel 4032 observations and the first guess equivalent using the final bias correction coefficients.

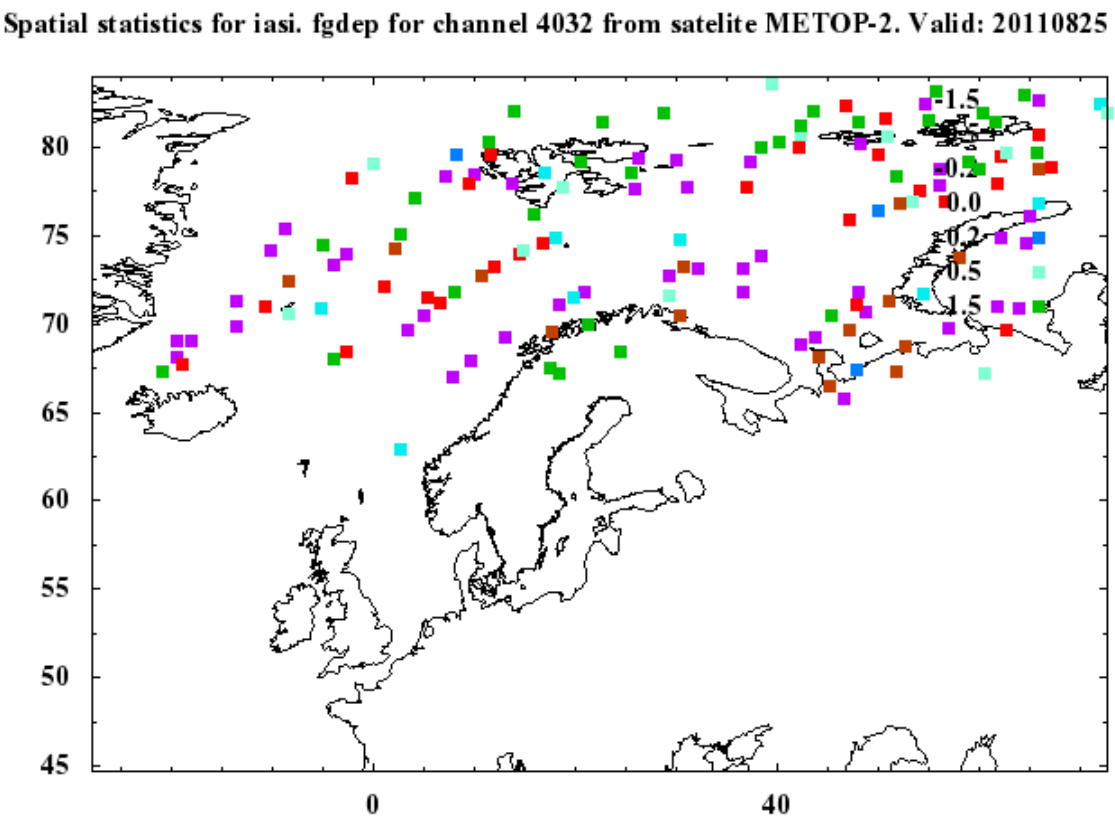

Figure 10: Departures from first guess field after bias correction for ch 4032 at same time as previous figures.

Figure 11 shows the geographical distribution of the departure between the IASI channel 4032 observations and the first analysis model equivalent. We note that the departures from the analysis are generally smaller than departures from first guess.

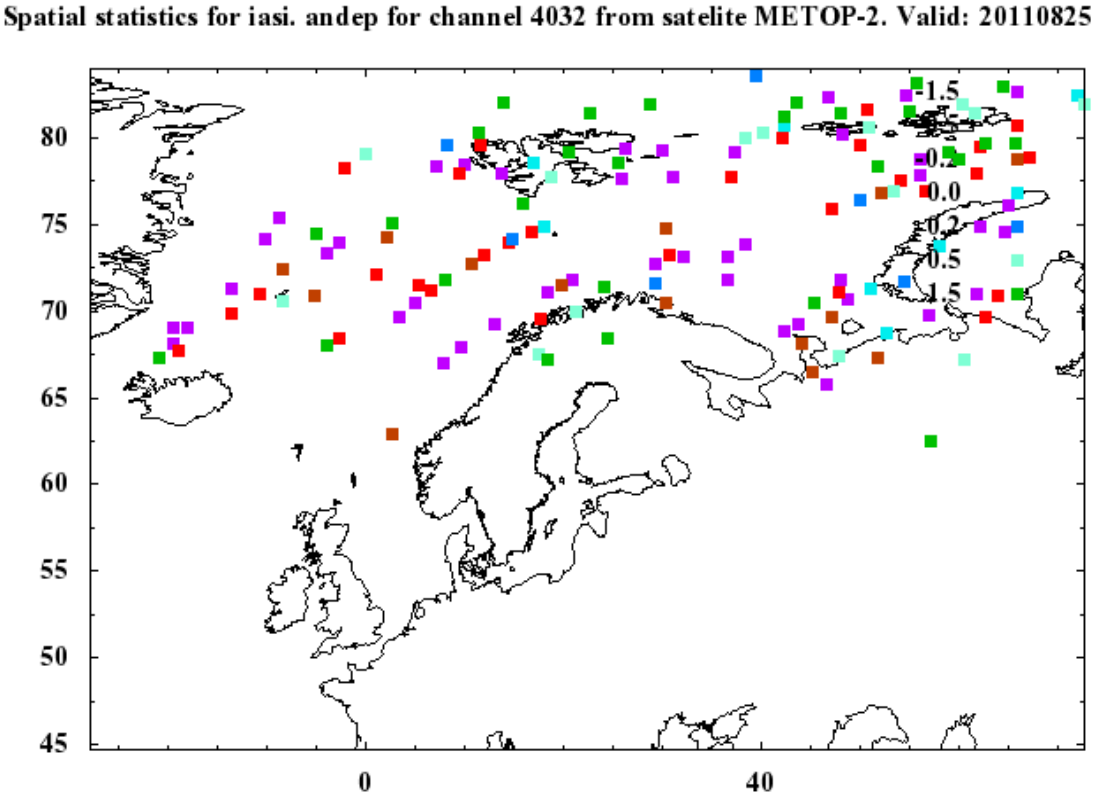

Figure 11: Departures from analysis field for ch 4032 at the same time as previous figures.

5 Overall verification results

Several verification tools are available at MET Norway to assess the quality of the forecasts. In this report we focus on verification against surface observations from the so called EWGLAM list, which is an internationally agreed set of observing stations believed to be of a good quality and therefore well suited for verification work.

The verification results of the two runs on wind, temperature and pressure, were virtually identical, which show that the added information from the moisture channels was small or was not interacting with the model dynamics to any large extent. However, we did see some differences in the precipitation verification, which was not unexpected, since we add information on a water-cycle variable.

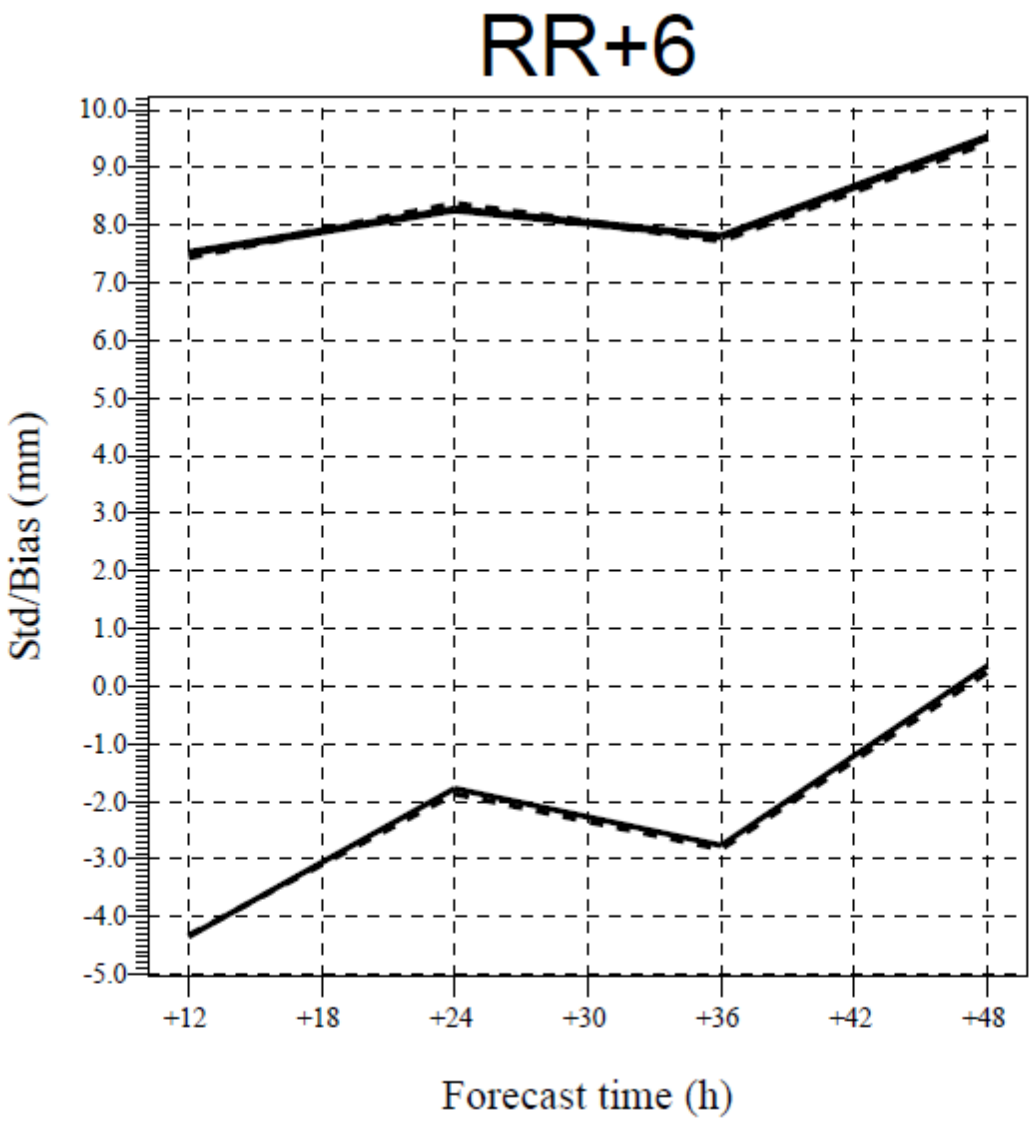

Figure 12: Verification of the forecast versus surface precipitation observations (6 hours accumulated precipitation). Solid line: The reference. Dashed line: The experiment with added water vapour channels.

InFigure 12 Figure 12 we observe some differences between the IASI experiment with water vapour channels (dashed) compared to the reference run without water vapour channels (solid lines). We do not see

a clear improvement from the water vapour channels here. However the next plot, Figure 13, has more weight to the short forecast ranges in the verification, and demonstrates some improvement.

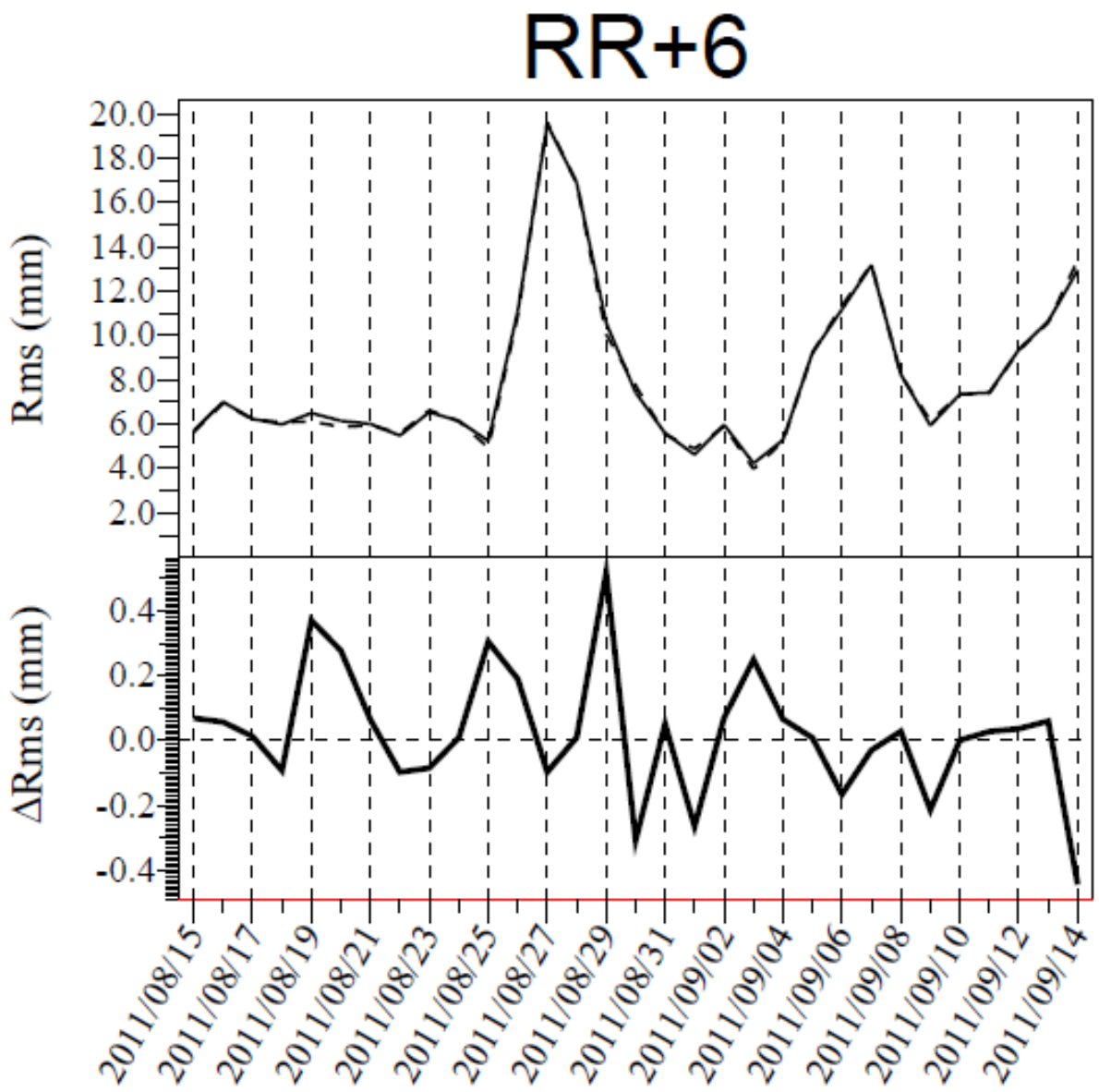

Figure 13: Timeseries of verification against precipitation observations (root mean square deviation, RMS). Upper curve: Dashed is the experiment with WV channels and solid line is the reference. The lower curve shows the differece between the two RMS values. Positive values indicate that the water vapour channels improve the forecast.

Figure 13 shows the time contribution to the 6 hours precipitation RMS. The verification is averaged over 6 hours intervals for all available forecast ranges and at each observation point in time. This represents a more smooth curve than if only one 6 hrs period should be considered. The lower curve shows the difference in the RMS, and it is defined so that the difference is positive when the IASI water vapour experiment scores better than the reference experiment. Data on the end of the period are only long forecasts and few samples relative to the other data in the timeseries so the apparent decrease in the verification score for the experiment at the end should not be given any significance.

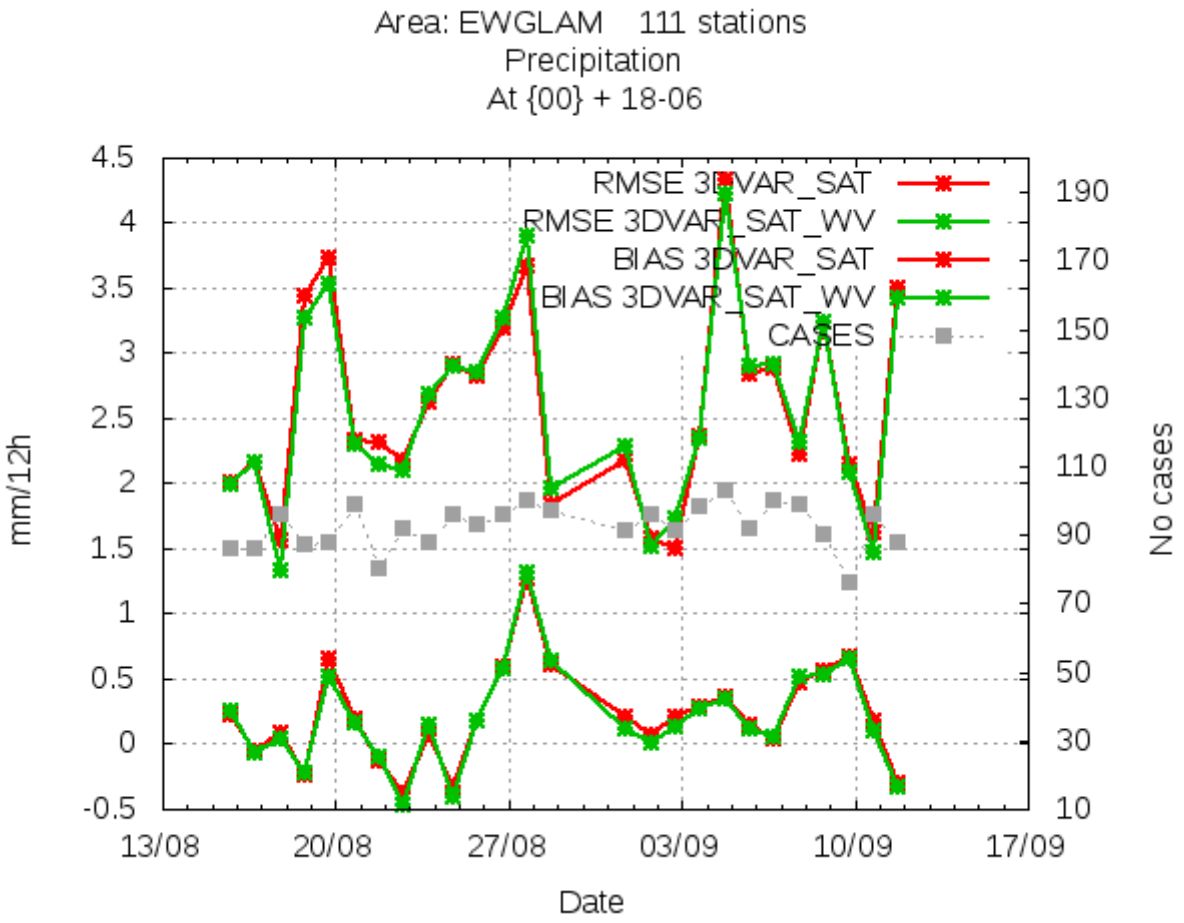

Figure 14: Timeseries of verification of 12 hours accumulated precipitation (starting at 6 and 18 hrs forecast range). Red is the reference and green is the water vapor channel experiment.

Figure 14 shows an alternative way of computing the time evolution of forecast quality, which is not as smooth in time as the previous figure. We can identify periods both where the reference run is better and where the experiment is better, but the periods where the water vapour channels gave an improvement seems to be longer and indicate an overall improvement.

Figure 15 shows an alternative way of verifying from the same dataset, using the Kuipers skill score, which indicates the quality of a forecast saying that the precipitation will exceed a certain threshold. This number is between -1 and +1 with higher numbers indicating better forecast quality, and the plots shows scores ofr a range of precipitation exceedance thresholds. Here we clearly see improvements of adding water vapour channels. The value at the high end of the precipitation scale represents very few samples, so the intermediate range where the water vapour experiment scores better is the most relevant.

In summary we find these verification results encouraging, particularly taking into account that we have chosen a relatively conservative approach in the channel usage. We do see, as one usually does in any observation impact study, a strong case to case variability, but the overall effect in this experiment seems to be on the positive side. The cases where we see apparent differences between the two runs and RMS errors in precipitation is large, are most likely when precipitation areas move over land where the density of EWGLAM stations is high. (Ocean is not well covered with precipitation observations.)

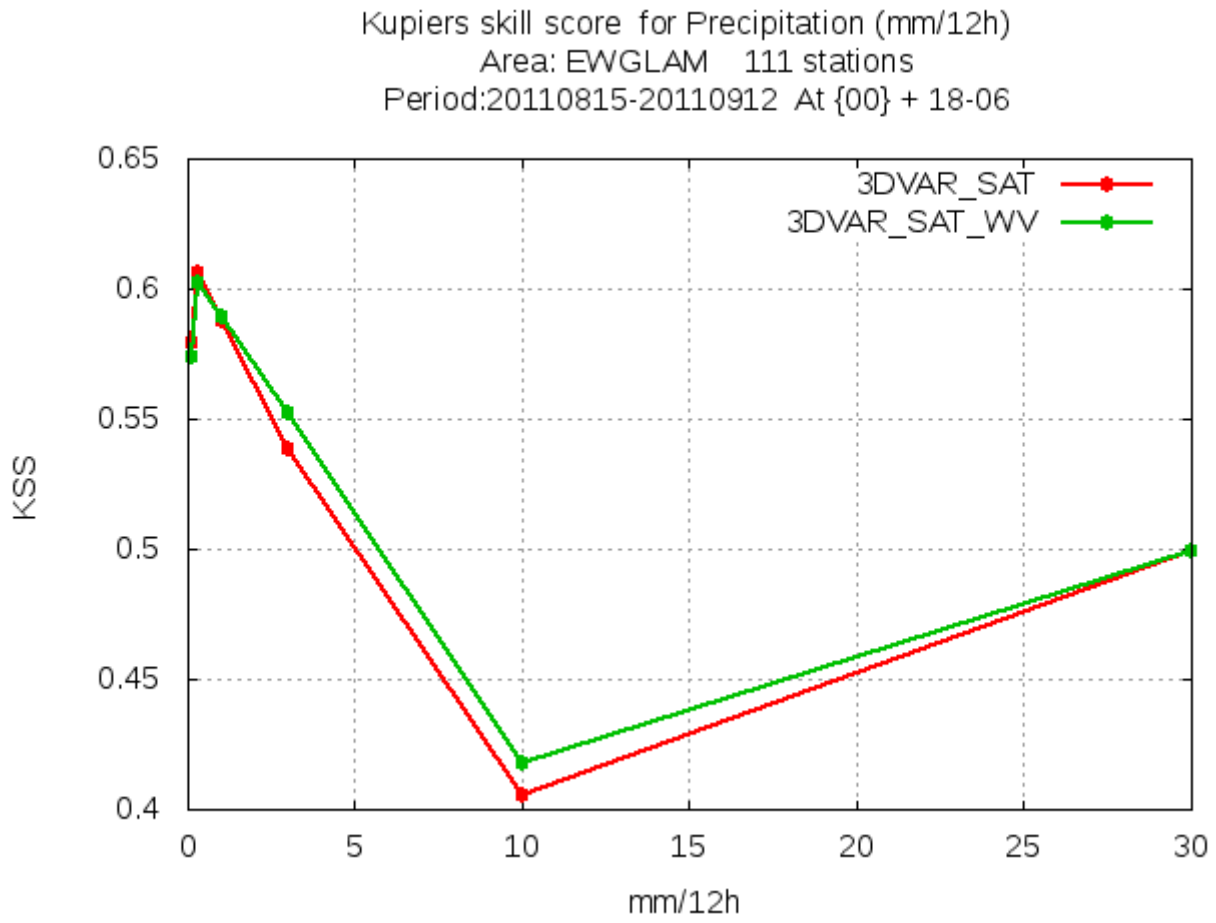

Figure 15: Kuipers skill score for exceendace of various thresholds of 12 hrs precipitation. This score takes values between -1 and +1, where higher value is better.

6 Case analysis

To study the effect of the added water vapor information in the experiments in more detail, we have assessed several precipitation events throughout the experiment period, and identified some events where the differences in the two suites were large. The first situation presented here is on 19 August, shown in Figure 16 and Figure 17. Here a strong precipitation area is affecting Southern Scandinavia and the Baltic. There are some strong differences between the two runs within this precipitation area, looking like a wave-like pattern with alternating positive and negative differences. This corresponds to moving cells of stronger precipitation within the precipitation area. One could speculate that positioning of smaller scale cells is a highly sensitive quantity and that a small perturbation in moisture thus has a relatively large effect. Within frontal precipitation areas one finds slantwise cells connected to symmetric instability. In areas with showers the instability is convective, and cells might be more separated and smaller and not as well aligned.

For the other three cases also presented here (Figure 18 to Figure 23), we see that there are similar effects. For the 29 Aug. and 31 Aug. cases, the precipitation seems more convective and cells smaller and more irregularly spread. The 4 Sept. case has a more regular difference structure, and one could speculate it is related to symmetric instability. We note that these perturbations in precipitation on average leads to better

forecast quality after adding the IASI moisture information according to the statistics of the preceding section.

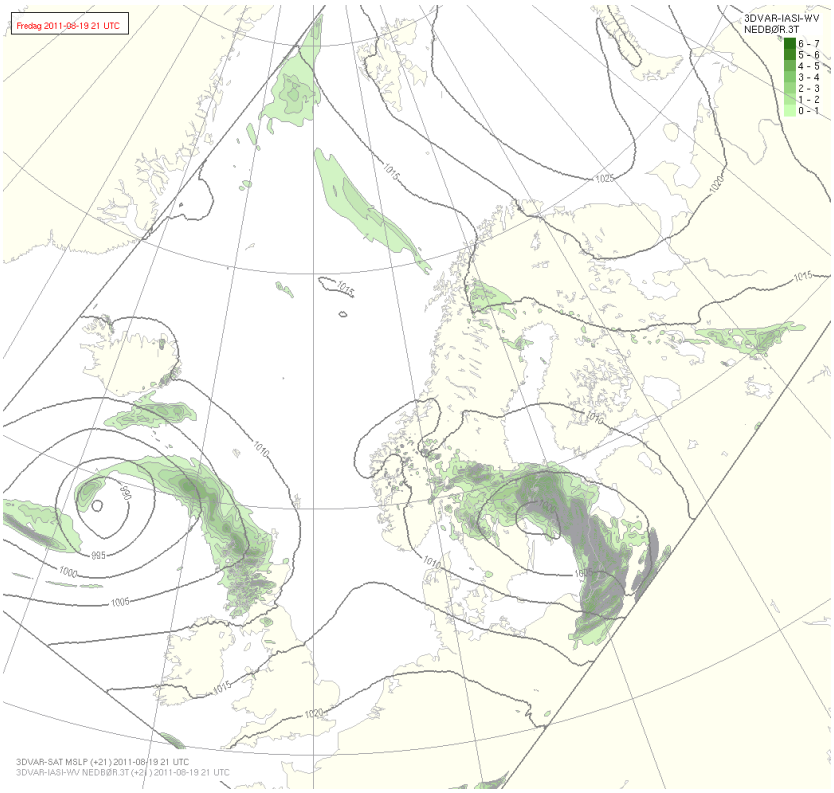

Figure 16: 3 hrs precipitation and pressure field from the experiment, 21 hours forecast valid 19 Aug 21 UTC.

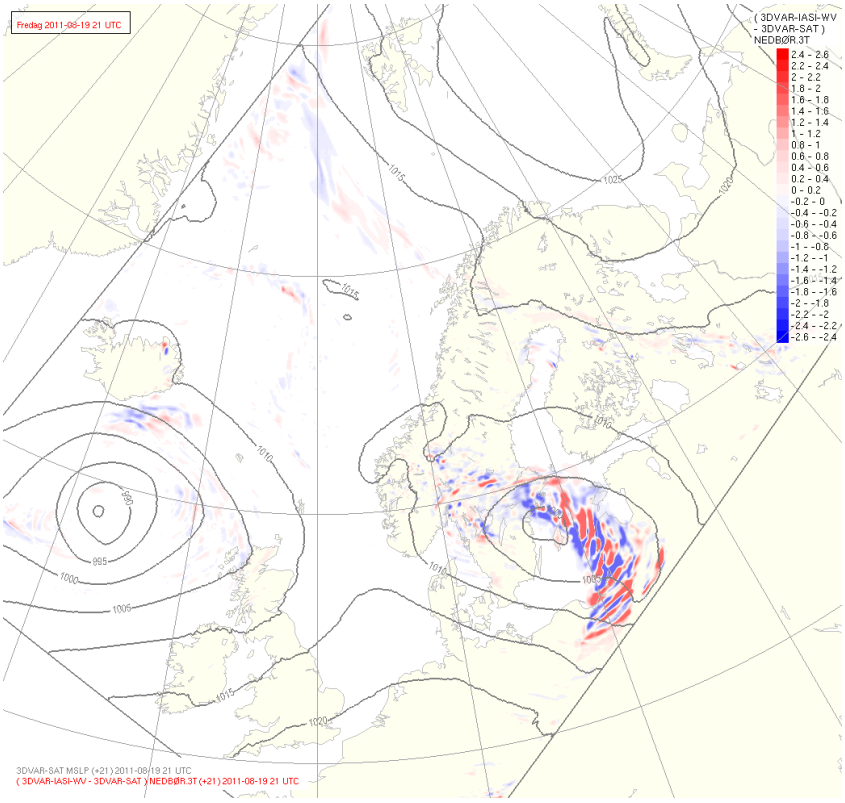

Figure 17: Difference in 3 hrs precipitation forecast between the experiment and reference run for the situation in Figure 16. Red colors indicate positive values (more precipitation in experiment), red is negative values.

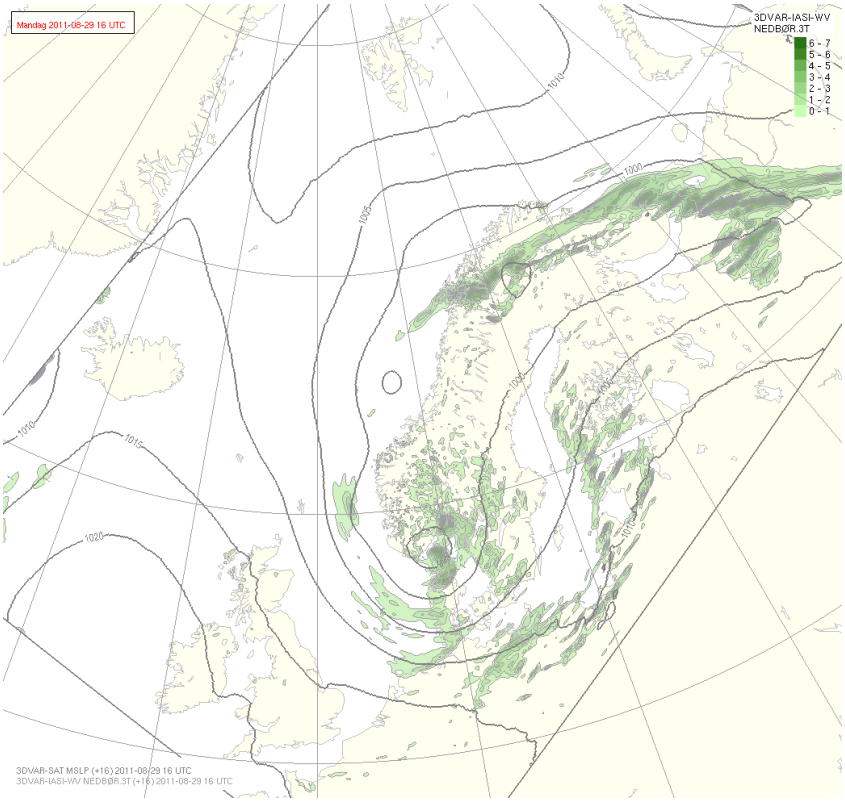

Figure 18: 3 hrs precipitation and pressure field from the experiment, 16 hours forecast valid 29 Aug 16 UTC.

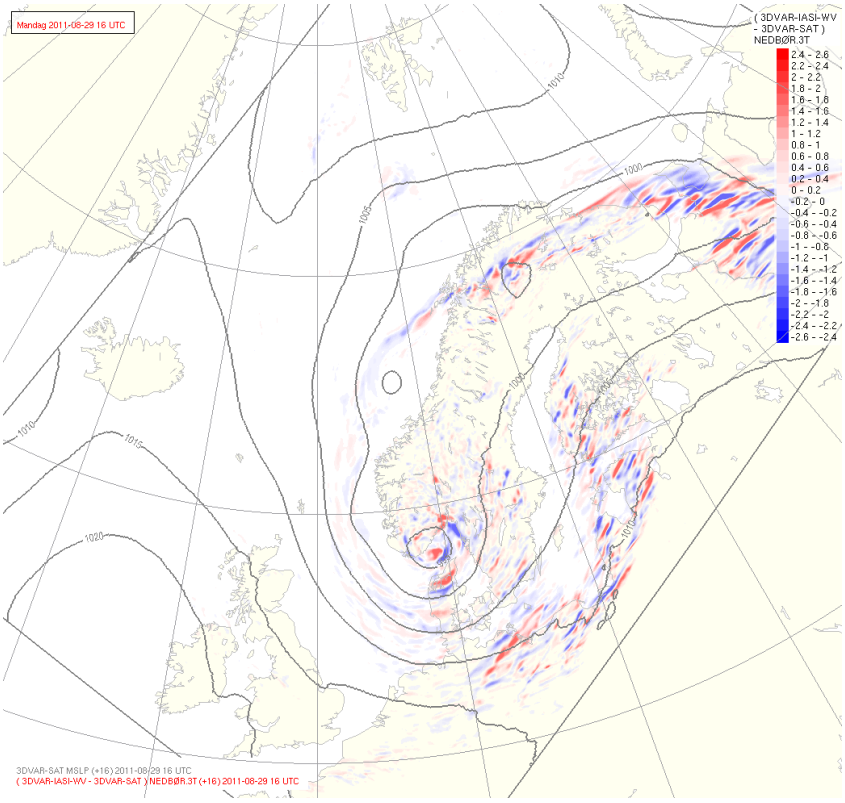

Figure 19: Difference in 3 hrs precipitation forecast between the experiment and reference run for the situation in Figure 18. Red colors indicate positive values (more precipitation in experiment), red is negative values.

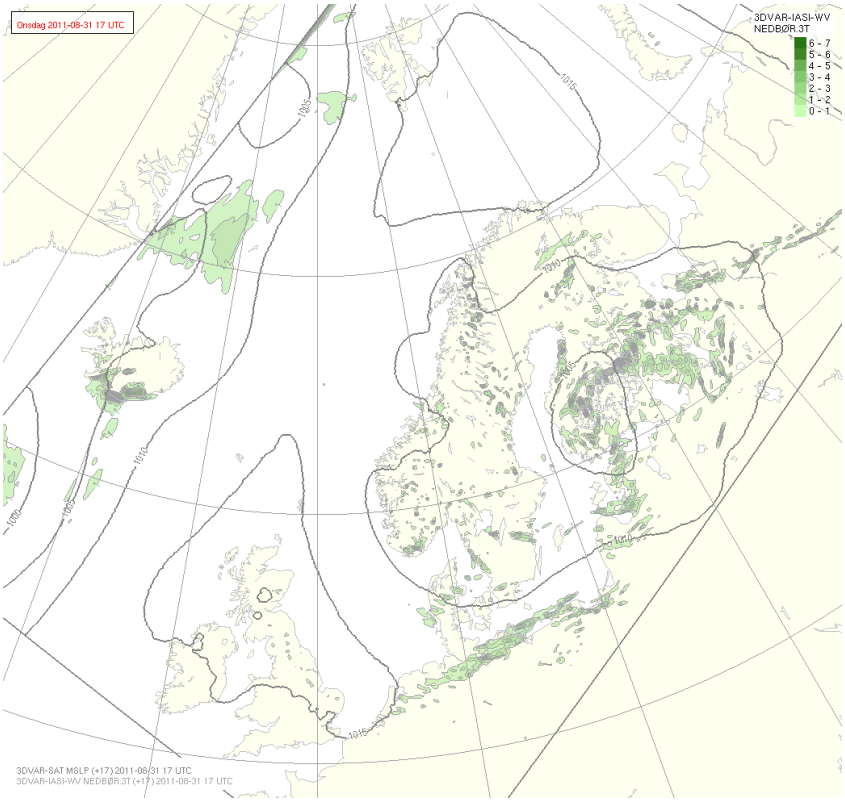

Figure 20: 3 hrs precipitation and pressure field from the experiment, 17 hours forecast valid 31 Aug 17 UTC.

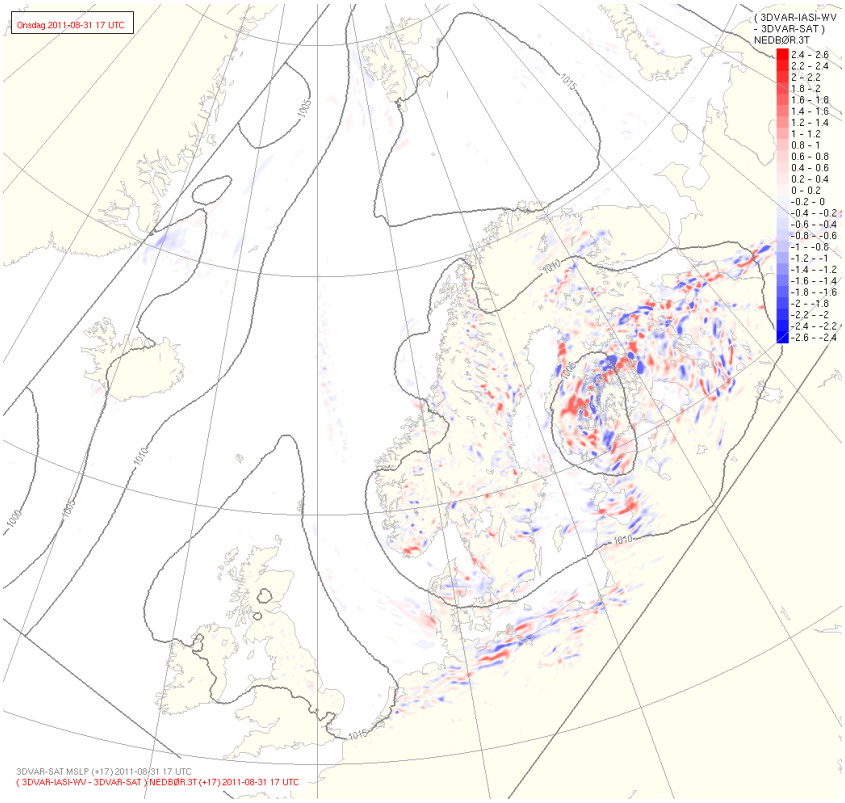

Figure 21: Difference in 3 hrs precipitation forecast between the experiment and reference run for the situation in Figure 20. Red colors indicate positive values (more precipitation in experiment), red is negative values.

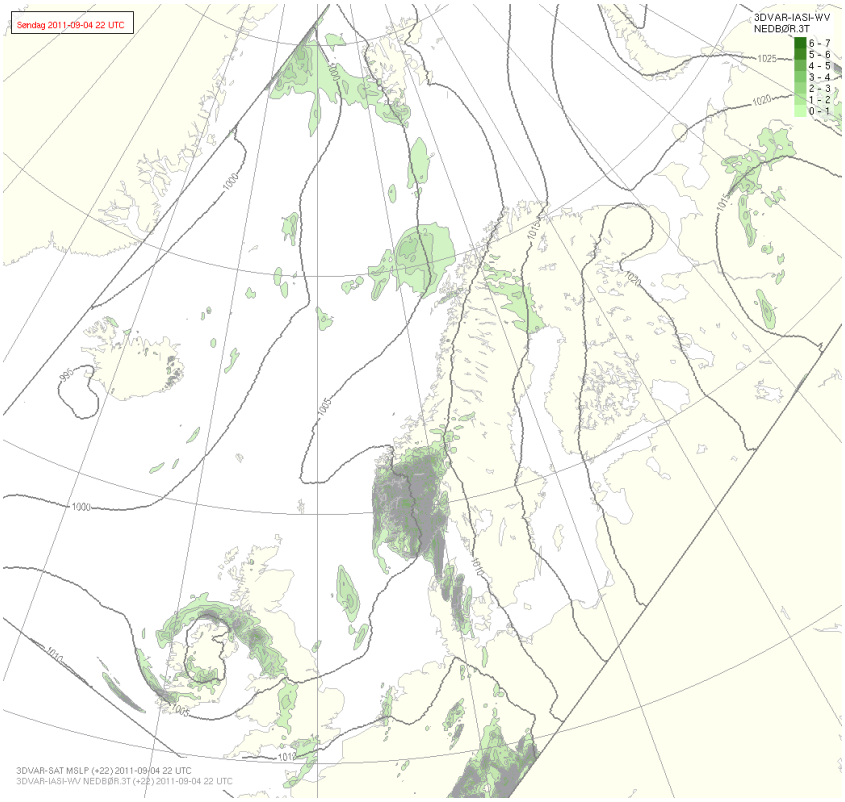

Figure 22: 3 hrs precipitation and pressure field from the experiment, 22 hours forecast valid 4 Sep 22 UTC.

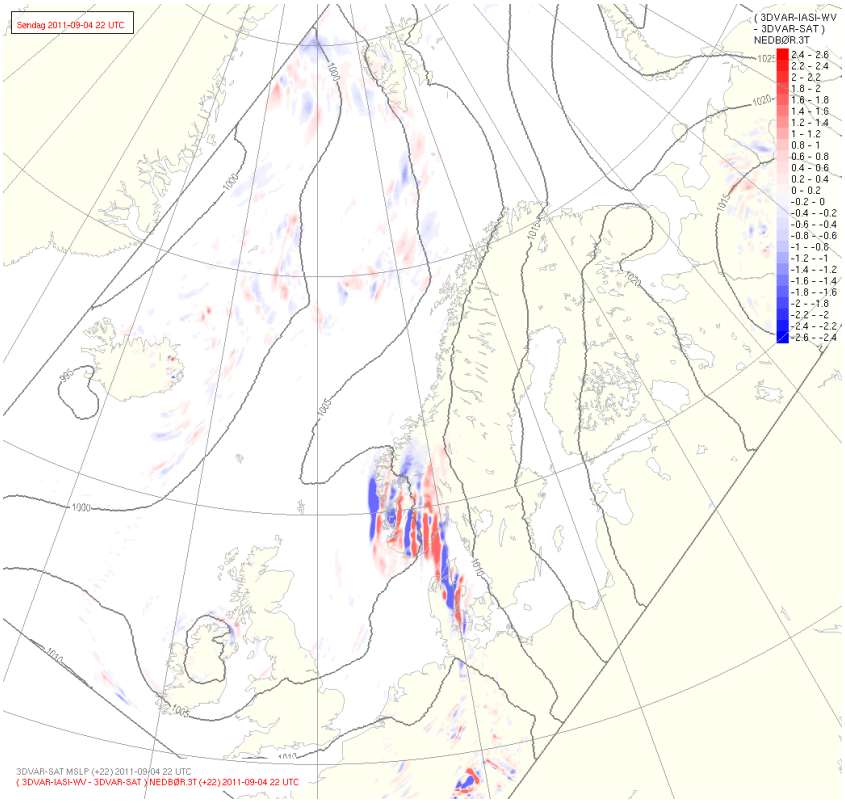

Figure 23: Difference in 3 hrs precipitation forecast between the experiment and reference run for the situation in Figure 22. Red colors indicate positive values (more precipitation in experiment), red is negative values.

7 Discussion and conclusions

The inclusion of moisture channels done here had very little effect on the atmospheric dynamics in terms of wind, temperature and pressure fields. A net positive impact of IASI moisture channels is seen on the precipitation verification, however highly variable and situation dependent. The moisture increments from IASI seem not to affect the average precipitation or the large-scale precipitation structures significantly, but it affects the positioning of precipitation cells.

The positive impact seen is encouraging, taking into account that a very conservative approach to channel usage was taken. It is still not clear whether the improvements are statistically significant, since the differences in the verification comes from a limited number of precipitation events.

So far only a first trial has been done, and further work is planned on optimizing the moisture channel usage, also including a larger number of channels including more data from the mid-troposphere.

References

Collard AD, McNally AP. 2009: The assimilation of Infrared Atmospheric Sounding Interferometer radiances at ECMWF. Q. J. R. Meteorol. Soc. 135: 1044–1058.

Matricardi M, Chevallier F, Kelly G, Thépaut J-N. 2004: An improved general fast radiative transfer model for the assimilation of radiance observations. Q. J. R. Meteorol. Soc. 130: 153–173.

Randriamampianina, R., F. Hilton and B. Candy, 2009: Improving the assimilation of the IASI and ATOVS data in polar region and limited area models. EUMETSAT Visiting Scientist Report, document NWPSAF-MO-VS-039, Version 1.0, 14 October 2009.

Randriamampianina, R., T. Iversen, and A. Storto, 2011: Exploring the Assimilation of IASI Radiances in Forecasting Polar Lows. Quarterly Journal of the Royal Meteorological Society, vol. 137, no 660, pp 1700–1715, October 2011.

Storto A and Randriamampianina R. 2010: The relative impact of meteorological observations in the Norwegian regional model as determined using an energy norm-based approach. Atmos. Sci. Let. 11: 51–58.

Appendix A: Bias plots for METOP-2 IASI Water Vapor channels

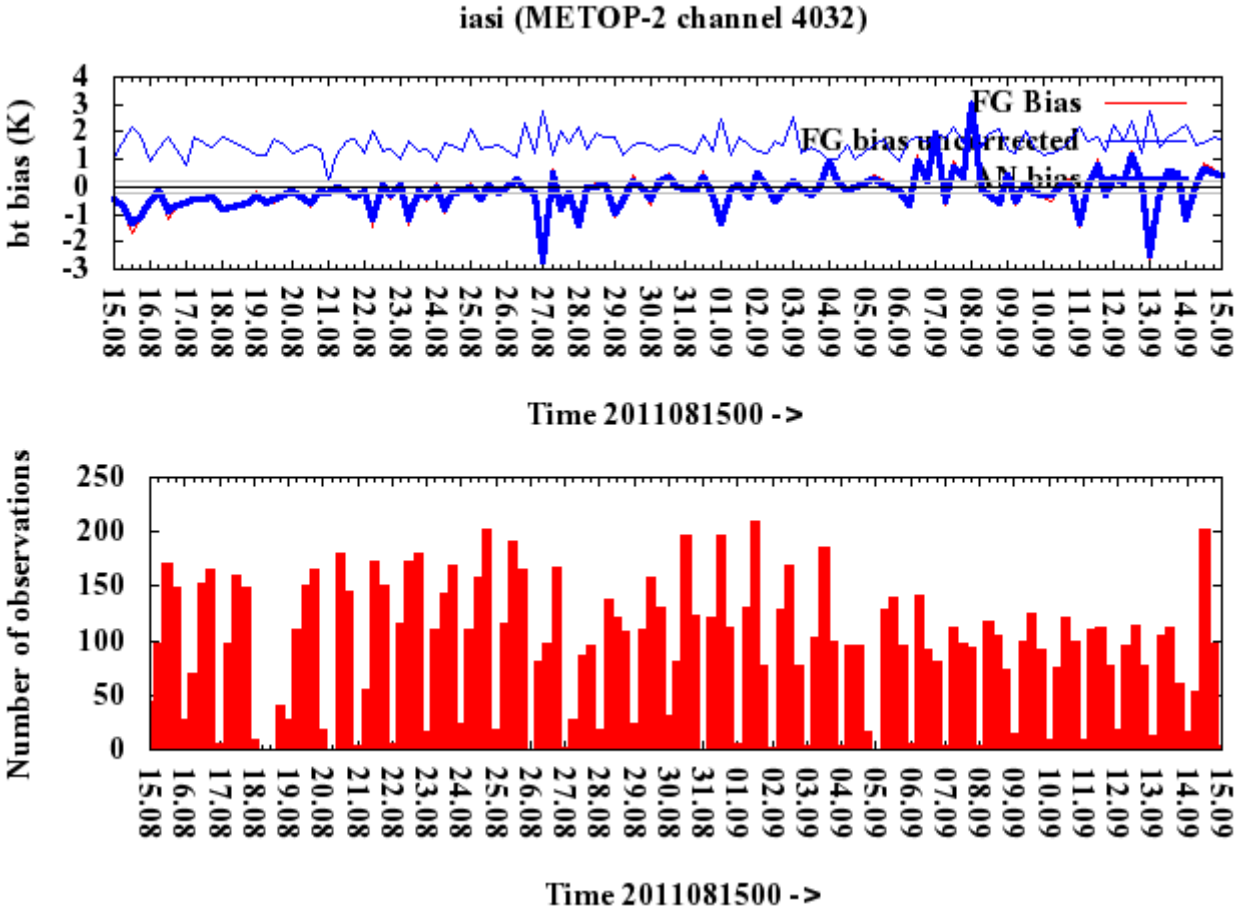

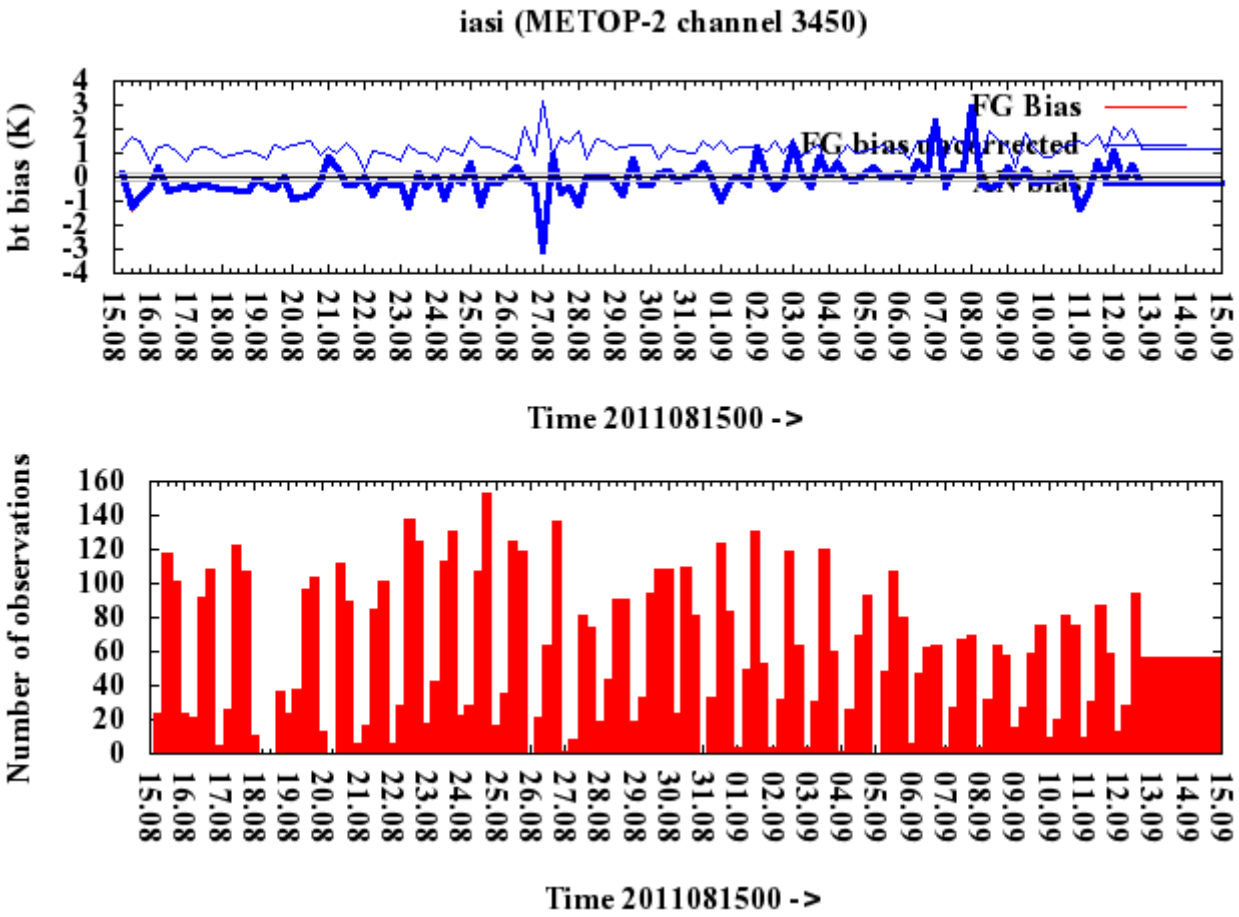
iasi (METOP-2 channel 3450)
bt bias (K)
FG Bias
FG bias uncorrected
AN bias
Time 2011081500 ->
Number of observations
Time 2011081500 ->

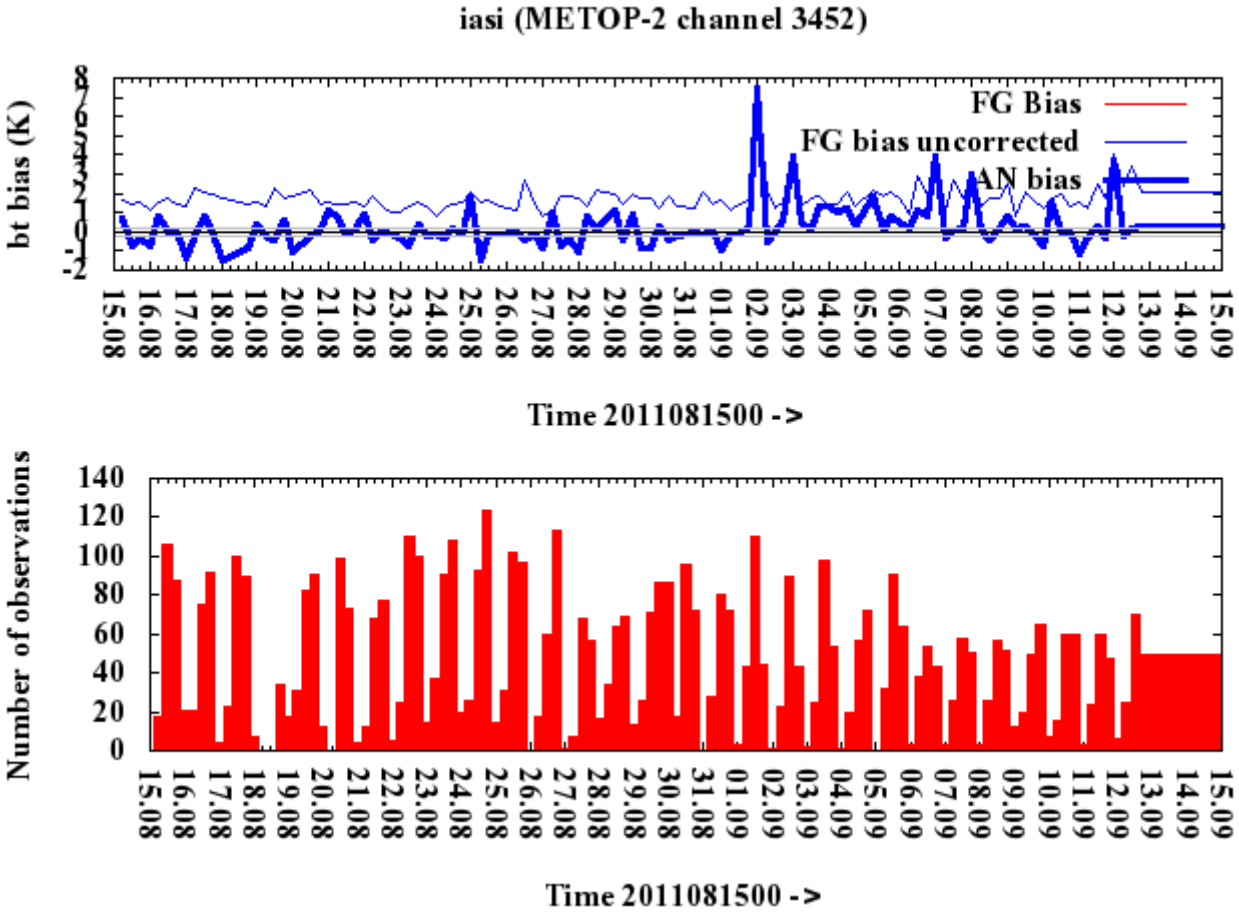
iasi (METOP-2 channel 3452)
bt bias (K)
FG Bias
FG bias uncorrected
AN bias
Time 2011081500 ->
Number of observations
Time 2011081500 ->

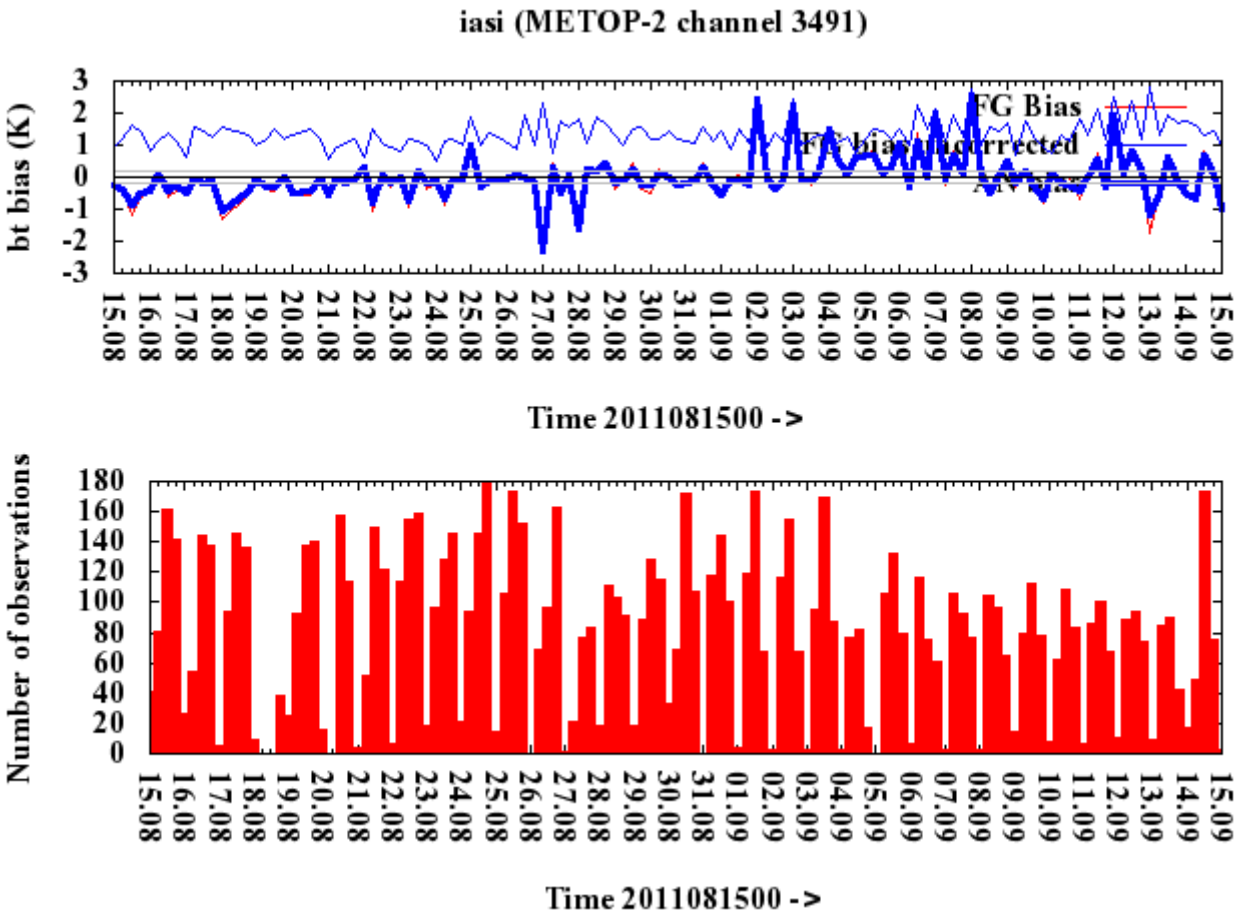
iasi (METOP-2 channel 3491)
bt bias (K)
FG Bias
FG bias uncorrected
Number of observations
Time 2011081500 ->
Time 2011081500 ->
iasi (METOP-2 channel 3506)
bt bias (K)
FG Bias
FG bias uncorrected
Number of observations
Time 2011081500 ->
Time 2011081500 ->
15.08
16.08
17.08
18.08
19.08
20.08
21.08
22.08
23.08
24.08
25.08
26.08
27.08
28.08
29.08
30.08
31.08
01.09
02.09
03.09
04.09
05.09
06.09
07.09
08.09
09.09
10.09
11.09
12.09
13.09
14.09
15.09

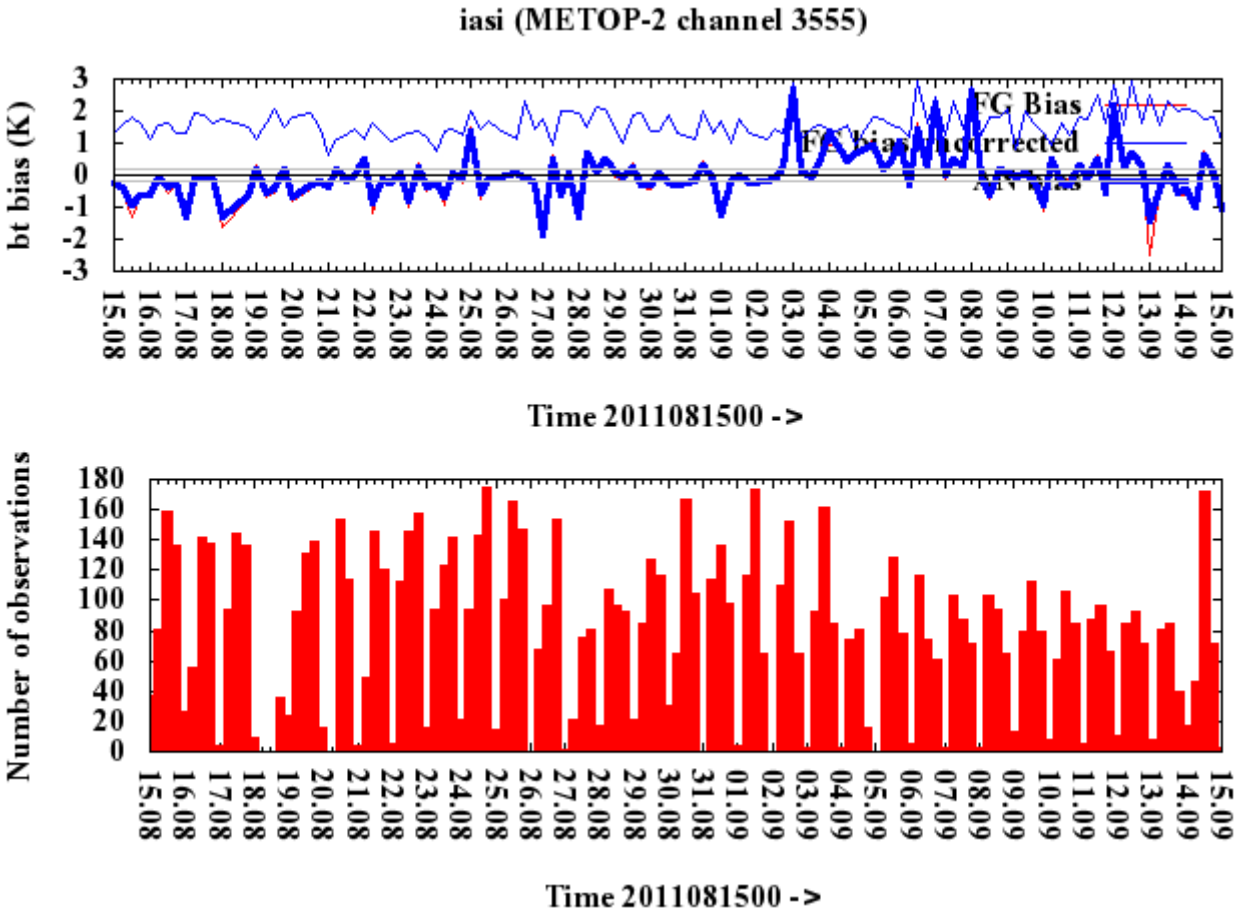
iasi (METOP-2 channel 3555)
bt bias (K)
FG Bias
Time 2011081500 ->
Number of observations
Time 2011081500 ->
iasi (METOP-2 channel 3575)
bt bias (K)
FG Bias
Time 2011081500 ->
Number of observations
Time 2011081500 ->
15.08
16.08
17.08
18.08
19.08
20.08
21.08
22.08
23.08
24.08
25.08
26.08
27.08
28.08
29.08
30.08
31.08
01.09
02.09
03.09
04.09
05.09
06.09
07.09
08.09
09.09
10.09
11.09
12.09
13.09
14.09
15.09

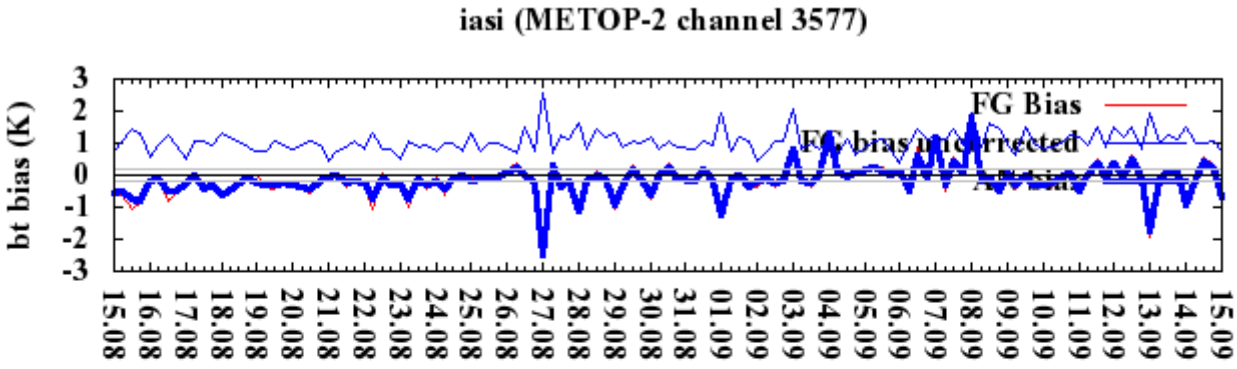
iasi (METOP-2 channel 3577)
bt bias (K)
FG Bias
FG bias uncorrected
Time 2011081500 ->
Number of observations
Time 2011081500 ->
iasi (METOP-2 channel 3580)
bt bias (K)
FG Bias
FG bias uncorrrected
Time 2011081500 ->
Number of observations
Time 2011081500 ->
15.08
16.08
17.08
18.08
19.08
20.08
21.08
22.08
23.08
24.08
25.08
26.08
27.08
28.08
29.08
30.08
31.08
01.09
02.09
03.09
04.09
05.09
06.09
07.09
08.09
09.09
10.09
11.09
12.09
13.09
14.09
15.09

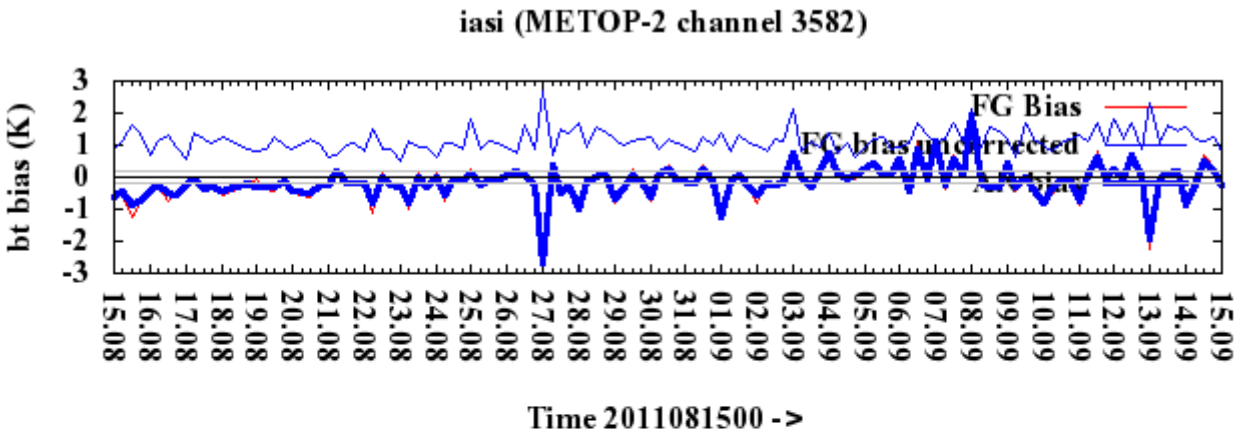
iasi (METOP-2 channel 3582)
bt bias (K)
FG Bias
FG bias uncorrected
Time 2011081500 ->
Number of observations
Time 2011081500 ->
iasi (METOP-2 channel 3589)
bt bias (K)
FG Bias
FG bias uncorrected
Time 2011081500 ->
Number of observations
Time 2011081500 ->
15.08
16.08
17.08
18.08
19.08
20.08
21.08
22.08
23.08
24.08
25.08
26.08
27.08
28.08
29.08
30.08
31.08
01.09
02.09
03.09
04.09
05.09
06.09
07.09
08.09
09.09
10.09
11.09
12.09
13.09
14.09
15.09

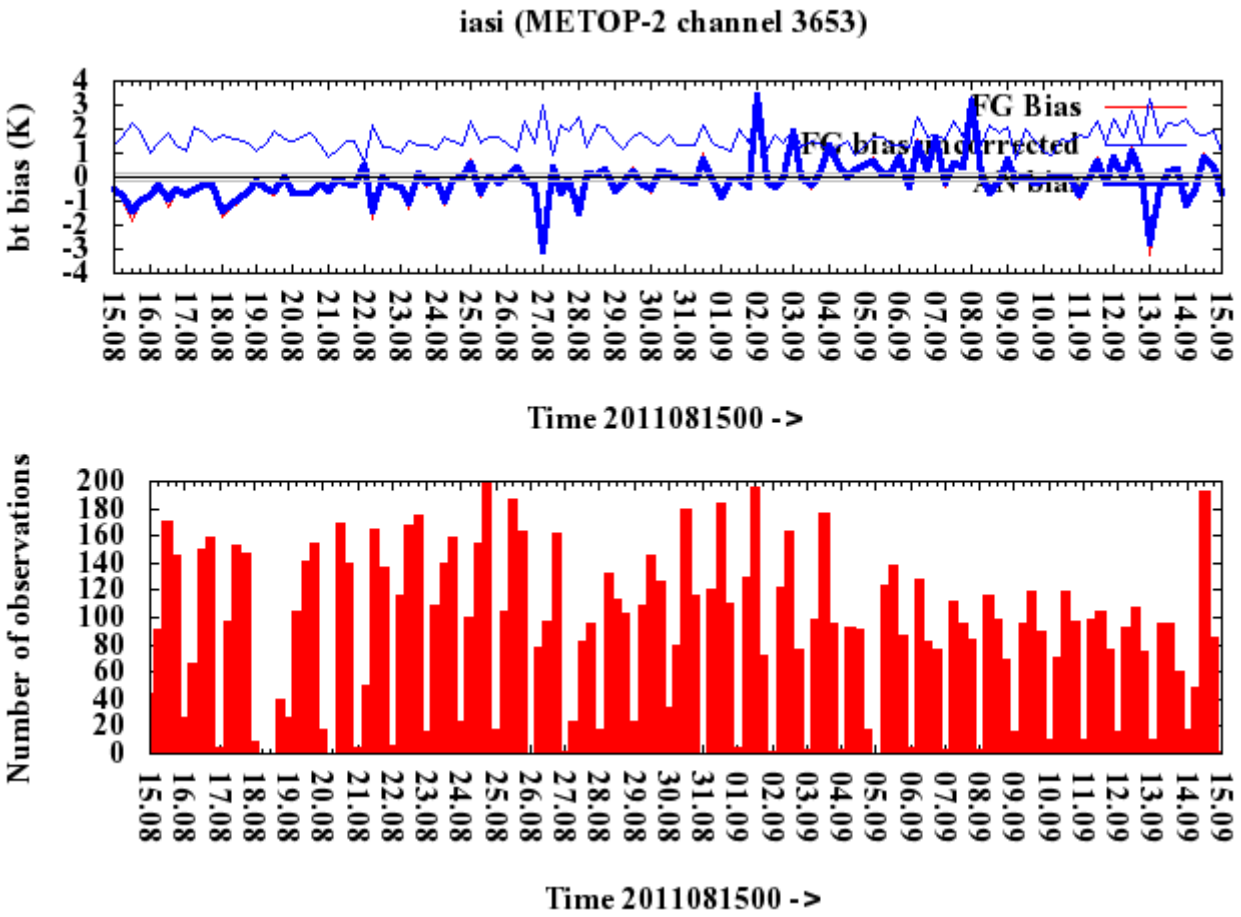
iasi (METOP-2 channel 3653)
bt bias (K)
FG Bias
FG bias uncorrected
Time 2011081500 ->
Number of observations
Time 2011081500 ->
iasi (METOP-2 channel 3658)
bt bias (K)
FG Bias
FG bias uncorrected
Time 2011081500 ->
Number of observations
Time 2011081500 ->
15.08
16.08
17.08
18.08
19.08
20.08
21.08
22.08
23.08
24.08
25.08
26.08
27.08
28.08
29.08
30.08
31.08
01.09
02.09
03.09
04.09
05.09
06.09
07.09
08.09
09.09
10.09
11.09
12.09
13.09
14.09
15.09

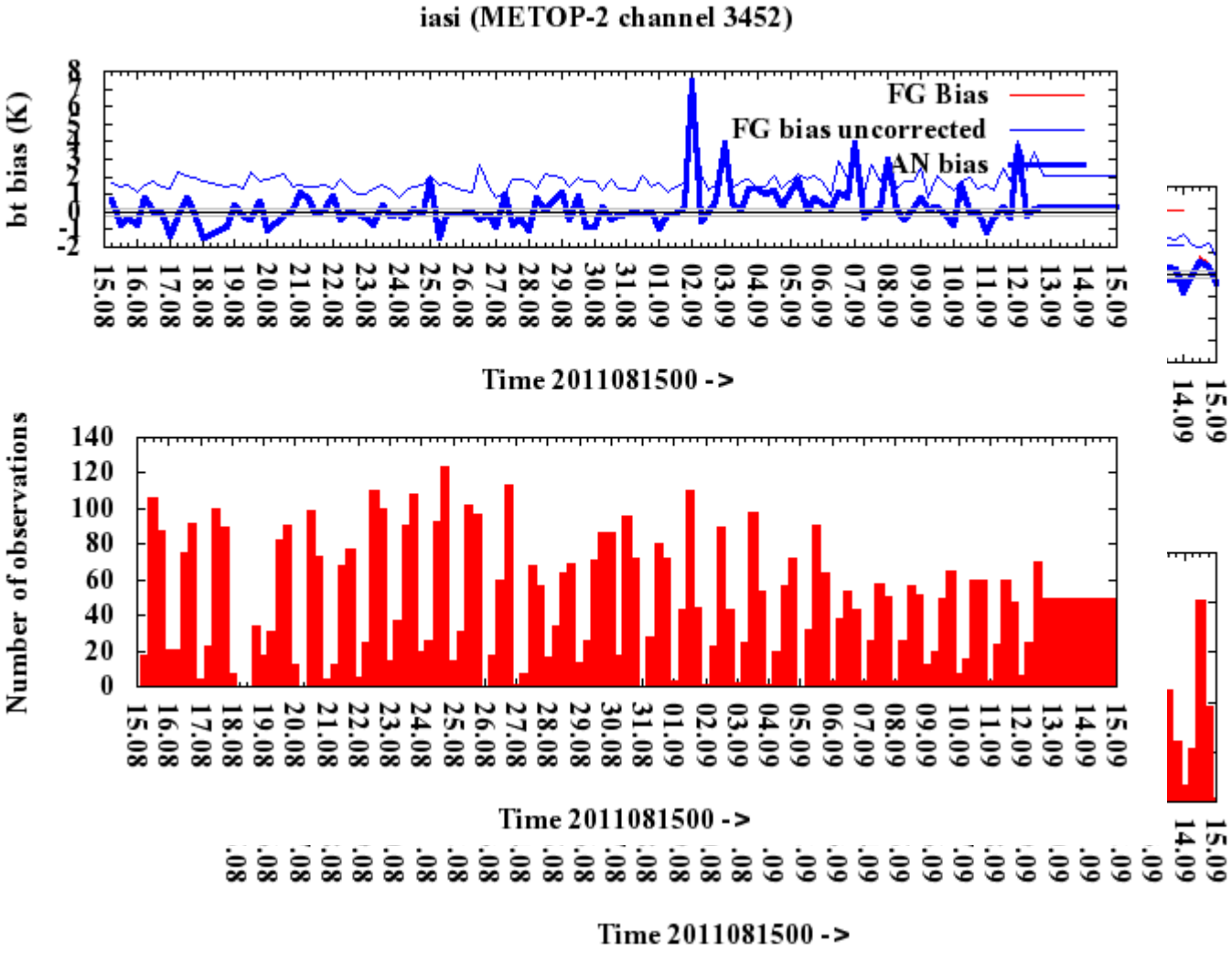
iasi (METOP-2 channel 3452)
bt bias (K)
FG Bias
FG bias uncorrected
AN bias
Time 2011081500 ->
Number of observations
Time 2011081500 ->
Time 2011081500 ->
iasi (METOP-2 channel 3448)
bt bias (K)
FG Bias
Time 2011081500 ->
Number of observations
Time 2011081500 ->
Time 2011081500 ->
15.08
16.08
17.08
18.08
19.08
20.08
21.08
22.08
23.08
24.08
25.08
26.08
27.08
28.08
29.08
30.08
31.08
01.09
02.09
03.09
04.09
05.09
06.09
07.09
08.09
09.09
10.09
11.09
12.09
13.09
14.09
15.09